Research Paper

PAIN®

Pro-opiomelanocortin neurons in the nucleus of the solitary tract mediate endorphinergic endogenous analgesia in mice

Pabitra Hriday Patra[a], Becks Tench[a], Timna Hitrec[a], Fiona Holmes[a], Robert Drake[a], Serena Cerritelli[b], David Spanswick[c], Anthony Edward Pickering[a,*]

Abstract

The nucleus of the solitary tract (NTS) contains pro-opiomelanocortin (POMC) neurons that are 1 of the 2 major sources of β-endorphin in the brain. The functional role of these NTS_{POMC} neurons in nociceptive and cardiorespiratory function is debated. We have shown that NTS_{POMC} optogenetic activation produces bradycardia and transient apnoea in a working heart–brainstem preparation and chemogenetic activation with an engineered ion channel (PSAM) produced opioidergic analgesia in vivo. To better define the role of the NTS_{POMC} neurons in behaving animals, we adopted in vivo optogenetics (ChrimsonR) and excitatory/inhibitory chemogenetic DREADD (hM3Dq/hM4Di) strategies in POMC-Cre mice. We show that optogenetic activation of NTS_{POMC} neurons produces time-locked, graded, transient bradycardia and bradypnoea in anaesthetised mice that is naloxone sensitive (1 mg/kg, i.p.), suggesting a role of β-endorphin. Both optogenetic and chemogenetic activation of NTS_{POMC} neurons produces sustained thermal analgesia in behaving mice that can be blocked by naloxone. It also produced analgesia in an inflammatory pain model (carrageenan) but not in a neuropathic pain model (tibial nerve transection). Inhibiting NTS_{POMC} neurons does not produce any effect on basal nociception but inhibits stress-induced analgesia (unlike inhibition of arcuate POMC neurons). Activation of NTS_{POMC} neuronal populations in conscious mice did not cause respiratory depression, anxiety, or locomotor deficit (in open field) or affective preference. These findings indicate that NTS_{POMC} neurons play a key role in the generation of endorphinergic endogenous analgesia and can also regulate cardiorespiratory function.

Keywords: β-Endorphin, Pro-opiomelanocortin, Nucleus of the solitary tract, Analgesia, Bradycardia, Bradypnoea, Optogenetics, DREADD chemogenetics

1. Introduction

Pro-opiomelanocortin (POMC) is the precursor of several important neuroactive peptides, including β-endorphin, α-melanocyte–stimulating hormone (α-MSH), and adrenocorticotropic hormone (ACTH).[7] Within the brain, POMC neurons are concentrated in only 2 regions: the arcuate nucleus of the hypothalamus (ARC) and the nucleus of the solitary tract (NTS) of the medulla.[3,6,53] In the mouse, there are approximately 3000 POMC neurons in the ARC, whereas the NTS contains 200 to 300 POMC neurons.[25] Multiple studies have reported a prominent role of ARC_{POMC} neurons in long-term regulation of feeding behaviour and energy homeostasis mediated by α-MSH.[3,6,53] In contrast, NTS_{POMC} neurons have been shown to have a short-term role in the regulation of feeding.[13,57]

Pro-opiomelanocortin neurons are also implicated in the regulation of nociception by the production of β-endorphin,[7,47] an endogenous opioid peptide that acts with high affinity at μ-opioid receptors.[16,35] β-Endorphin has been linked to the "opioid burn" analgesia of exercise,[9,12,38,45] and it is causally involved in the mediation of stress-induced analgesia.[47] In addition to its role in analgesia, β-endorphin is also reported to be involved in reward processing,[51] sexual behaviour,[4] and cardiorespiratory control.[32]

Although this evidence indicates that central β-endorphin has roles in the mediation of endogenous analgesia and cardiorespiratory control, the circuit mediation of these roles is less clearly defined. More attention has focussed on the hypothalamic ARC_{POMC} neurons and the involvement of NTS_{POMC} neurons in these actions is still debated. We previously demonstrated that chemogenetic activation of POMC neurons (using the pharmacologically selective actuator module [PSAM] strategy[33]) produces analgesia in vivo in the tail-flick assay.[13] We also showed that optogenetic activation of NTS_{POMC} neurons produces marked bradycardia and bradypnoea in the working heart–brainstem preparation.[13] These cardiorespiratory depressant effects were produced by short synchronous

Sponsorships or competing interests that may be relevant to content are disclosed at the end of this article.

[a] Anaesthesia, Pain and Critical Care Research, School of Physiology, Pharmacology and Neuroscience, University of Bristol, Bristol, United Kingdom, [b] Radcliffe Department of Medicine, University of Oxford, John Radcliffe Hospital, Oxford, United Kingdom, [c] Neurosolutions, University of Warwick, Coventry, United Kingdom

**Corresponding author. Address: Anaesthesia, Pain and Critical Care Research, School of Physiology, Pharmacology and Neuroscience, University of Bristol, Bristol BS8 1TD, United Kingdom. Tel.: 144 117 3312311. E-mail address: Tony.Pickering@bristol.ac.uk (A. E. Pickering).*

Supplemental digital content is available for this article. Direct URL citations appear in the printed text and are provided in the HTML and PDF versions of this article on the journal's Web site (www.painjournalonline.com).

PAIN 164 (2023) 1051–1066

© 2022 International Association for the Study of Pain

http://dx.doi.org/10.1097/j.pain.0000000000002802

Copyright © 2022 by the International Association for the Study of Pain. Unauthorized reproduction of this article is prohibited.

bursts of optoactivation in a decerebrate preparation. Such cardiorespiratory depressant actions could compromise the potential analgesic utility of their selective activation. However, it was unclear how more physiological modulation of activity of the NTS_{POMC} neurons would influence the regulation of heart rate and respiration in vivo.

In an initial pilot investigation using assays of respiration to address this question, we found that the chemogenetic ligand $PSEM^{89S}$ (90 mg/kg) also had effects in control mice. We therefore designed the present study using excitatory optogenetics[56] and DREADD-mediated chemogenetics[46] to test whether NTS_{POMC} neuronal activation in mice in vivo is analgesic in acute, inflammatory, and neuropathic pain models or has cardiorespiratory depressant effects. We extended our study to assess the role of these neurons in mediating stress-induced analgesia using an inhibitory DREADD-mediated subtractive chemogenetic strategy.

2. Materials and methods

All procedures followed the UK Animals (Scientific Procedures) Act of 1986 and were approved by the University of Bristol Animal Welfare and Ethical Review Board.

2.1. Animals

Experiments were conducted on adult male and female transgenic POMC-Cre mice[5] bred and housed in the animal facility at the University of Bristol. All mice were maintained in 12h:12h light:dark cycle, a room temperature of 20 ± 1°C, and humidity of 50 ± 10%, with ad libitum access to food and water. We did not have any sex-specific hypotheses for the study, and both male and female mice were randomly allocated to experimental groups. The surgical procedures, viral vector injections, and behavioural testing conducted on each group of mice are detailed in Supplementary Table 1 (available at http://links.lww.com/PAIN/B733).

2.2. Viral vectors

The following adeno-associated viral vectors (AAVs) were used in the study to express optogenetic and chemogenetic actuators in POMC neurons.

AAV-ChrimsonR-tdTomato[29] (AAV-Syn-FLEX-rc[ChrimsonR-tdTomato], gift from Edward Boyden, serotype AAV5; titre 1.1×10^{13} GC/mL; Addgene vector prep #62723) was microinjected in the NTS for optogenetic experiments producing $NTS_{POMC(Chrim)}$ mice.

AAV-hM3Dq-mCherry[30] (AAV-hSyn-DIO-hM3D(Gq)-mCherry, gift from Bryan Roth, serotype AAV2, titre 2×10^{13} GC/mL, Addgene USA, viral prep # 44361-AAV2) was microinjected for excitatory chemogenetic experiments producing $NTS_{POMC(Gq)}$ mice.

AAV-hM4Di-mCherry (rAAV2/hsyn-DIO-hM4D(Gi)-mCherry, titre 4.6×10^{12} GC/mL; Addgene USA) was microinjected to the NTS or ARC for inhibitory chemogenetic experiments producing $NTS_{POMC(Gi)}$ and $ARC_{POMC(Gi)}$ mice, respectively.

AAV-hSyn-FLEX-PSAM-$5HT_3$ (stock viral titre 2.8×10^{12} GC/mL, diluted 1:10 with sterile PBS; Scott Sternson, Janelia Research Campus, VA) was microinjected into the NTS of POMC-Cre mice[13] producing $NTS_{POMC(PSAM)}$ mice.

AAV-EF1α-DIO-ChR2-mCherry (UNC Vector Core Services, Chapel Hill, NC; 6×10^{12} viral particles/mL) was injected for control experiments for the PSAM spirometry experiments.

2.3. Viral vector injection and optic fibre implantation

Recovery surgery for vector injection was performed under general anaesthesia with ketamine (70 mg/kg, i.p.) and medetomidine (0.5 mg/kg, i.p.). Two approaches were taken for viral vector injections that yielded similar patterns of transduction.

For the majority of studies, the viral vector was injected into the medulla via the atlanto-occipital foramen as per Cerritelli et al.[13] In brief, the mouse was positioned in a stereotaxic frame with its head angled down 20° from the horizontal. A small midline skin incision was made from the occiput down over the neck. The neck muscles were parted to reveal the atlanto-occipital membrane that was incised to get a view of area postrema. Calamus scriptorius, located on the dorsal surface of the medulla, was used as the reference for the stereotaxic injections. A vector-filled pulled glass pipette was placed at the rostro-caudal level of the tip of calamus scriptorius, 0.2 mm lateral to the midline and at a 35° angle to the vertical. Vector injections (180 nL over 2 minutes) were made unilaterally at 4 sites (0.25, 0.50, 0.75, and 1.00 mm) below the surface of the medulla.

For the chronically implanted optogenetic studies in behaving mice, a trans-cerebellar approach was used for the NTS vector injections as this provided a better skull anchorage for the optic fibre. The anaesthetised mouse was placed in the stereotaxic frame with the skull level and a 1-mm-diameter burr hole was made (−7.5 mm anterior-posterior [AP] and 0.2 mm medio-lateral [ML] from bregma). The AAV was injected at 4 sites along a vertical track (180 nL at each site located 3.25, 3.5, 3.75, and 4 mm below the cerebellar surface). The optic fibre was implanted during the surgery at the same co-ordinates to a depth of 4 mm below the cerebellar surface (Lambda-B fibre 0.66NA, 200 μm core diameter, emitting length 2 mm, implant length = 5 mm; Optogenix, Arnesano, Italy). These optical fibre implants are advantageous because of the emission along the length of the taper as well as from the tip that illuminates a large volume of tissue in vivo.[43] Additionally, the large numerical aperture (0.66) efficiently collects the light from the light emitting diode (LED), and its penetration into the tissue is enhanced by the longer wavelength of light (620 nM) used for activation of the red-shifted excitation spectrum of the optimised opsin ChrimsonR[29] compared with ChannelRhodopsin2. A stainless steel anchoring screw was implanted over the occiput and the fibre was fixed with dental cement (Dental Reline, United Kingdom).

For the hypothalamic ARC injections, anaesthetised mice were placed in a stereotaxic frame, the skull was levelled, the cranial surface was exposed, and two 1-mm-diameter burr holes were made (−1.5 mm AP and ±1 mm ML from bregma). The injecting micropipette was angled 10° towards the midline and the appropriate AAV was injected at 4 sites along a vertical track (180 nL at 5.6, 5.8, 6.0, and 6.2 mm below the cerebellar surface).

Once the injection/implantation was completed, the skin edges were sutured closed and antiseptic wound powder was applied. Mice were given atipamezole (1 mg/kg, i.p.) to reverse the anaesthesia and buprenorphine (0.1 mg/kg, s.c.) for analgesia. All experiments were conducted at least 3 weeks after AVV injection.

2.4. Acute medullary slice electrophysiology

At 3 to 5 weeks after AAV injection, the $NTS_{POMC(Chrim)}$ mice were terminally anaesthetised using isoflurane (5%), then decapitated. The brainstem was dissected free and submerged in ice-cold, carbogenated, slicing artificial cerebrospinal fluid (ACSF) containing (mM) 26 $NaHCO_3$, 1.2 KH_2PO_4, 1.9 KCl, 0.4 $CaCl_2$, 3.9 $MgCl_2$, 10 glucose, 154 sucrose, and 0.34 ascorbic acid. Coronal

Copyright © 2022 by the International Association for the Study of Pain. Unauthorized reproduction of this article is prohibited.

slices of medulla were cut in the ventral to dorsal direction (300 μm thick). Slices rested at 34°C for 30 minutes in cutting solution before being transferred to recording ACSF of the same temperature for a further 30 minutes before being kept at 20°C. Recording ACSF contained (mM) 126 NaCl, 26 $NaHCO_3$, 1.25 NaH_2PO_4, 2.5 KCl, 2 $CaCl_2$, 2 $MgCl_2$, and 10 glucose at pH 7.3.

Visualised patch clamp recordings were obtained from slices in a heated bath (34°C) perfused with ACSF at 2.5 mL/minute on the stage of a Leica DMLFSA microscope. Neuronal profiles were visualised with Dodt gradient contrast. Epifluorescence illumination from a mercury light source via filter cube (N2.1, excitation filter 515-560 nm) was used to visualise the tdTomato in labelled neurons and axonal projections within the slice (**Fig. 1A**). Patch pipettes were pulled from thin wall filamented glass (Harvard Apparatus, Cambridge, United Kingdom; GC120F-10). They were filled with internal solution containing (mM) 130 K-gluconate, 10 KCl, 10 Na-HEPES, 0.2 EGTA, 4 MgATP, and 0.3 Na_2GTP, pH 7.3 and 310 mOsm. Filled pipettes had a tip resistance of 6 to 9 MΩ. Illumination for optogenetic activation was delivered from a 620-nm LED (11 mW PlexBright module; Plexon, Dallas, TX) coupled to a 200-μm-diameter optic fibre placed above the target cells.

Current/voltage clamp recordings were made with a Multiclamp 700A patch amplifier (Axon Instruments, San Jose, CA) controlled by Multiclamp 700A commander software. Data were low pass filtered at 3 kHz before being sampled at 10 kHz (Micro 1401; Cambridge Electronic Design) to enable acquisition in Spike (v7) or Signal (v5). WinWCP (V5.2.0) (John Dempster, University of Strathclyde, United Kingdom) was used for analysis of photocurrents. Figures were created in Inkscape (v0.48), ImageJ (v1.51), and OriginPro (v2018b).

2.5. Cardiorespiratory recordings in vivo

2.5.1. Acute optogenetic activation of NTS_{POMC} neurons in anaesthetised mice

Electrocardiogram (ECG) and thoracic respiratory muscle electromyogram (EMG) were recorded under anaesthesia (urethane 0.8 g/kg, i.p., n = 3 mice) to assess the effect of opto-stimulation on heart rate and respiration, respectively, in $NTS_{POMC(Chrim)}$ mice. Needle electrodes (23-gauge) were inserted subcutaneously into the animal over the chest. The electrodes were connected to custom-built AC amplifier (x5-10K, PPN electronic workshop, University of Bristol).

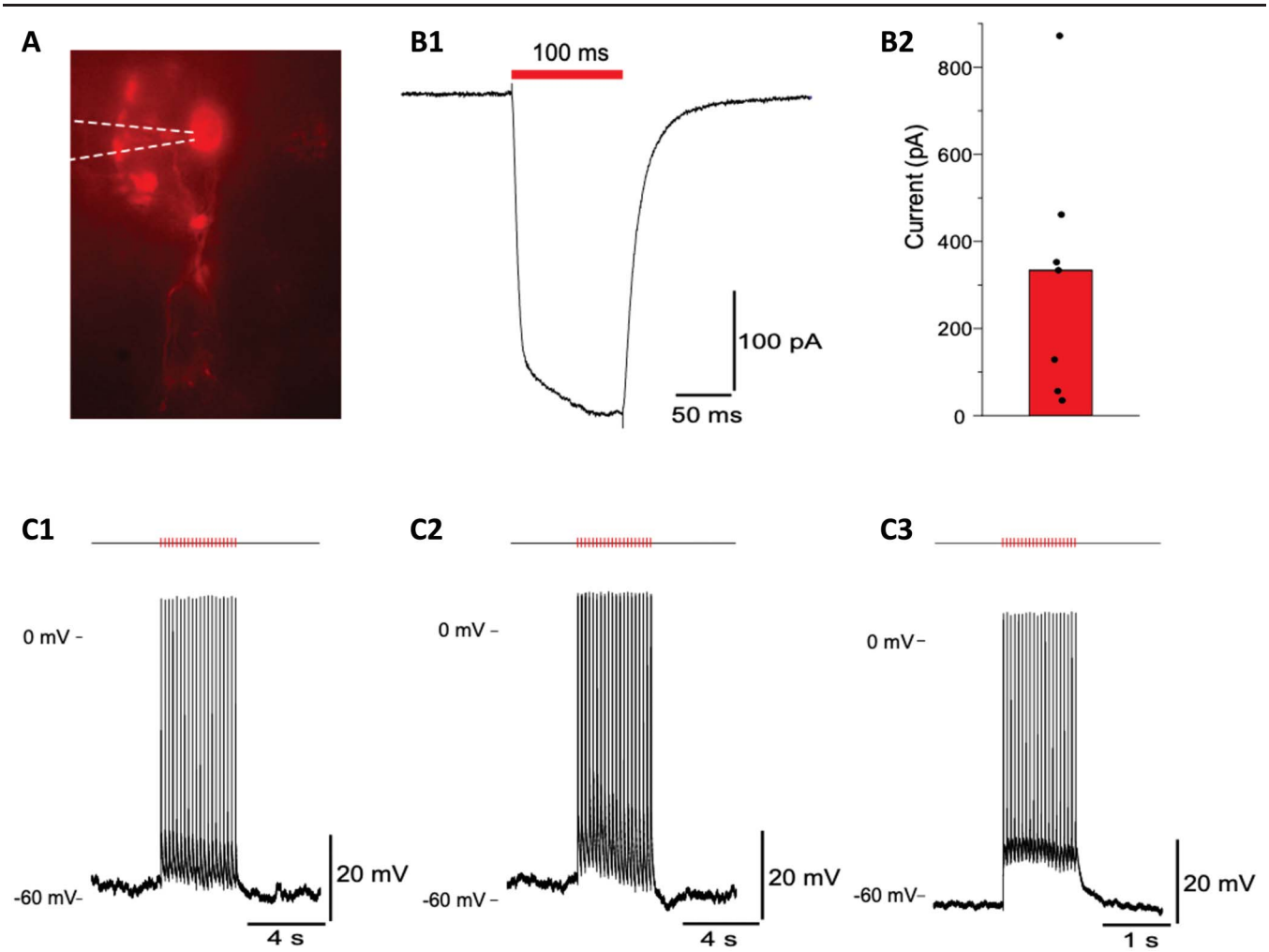


Figure 1. Optogenetic activation of NTS_{POMC} neurons expressing ChrimsonR. (A) Example ChrimsonR-tdTomato–positive POMC neuron in an acute medullary slice targeted for whole-cell patch clamp recordings. Dashed lines indicate pipette location. (B_1) ChrimsonR-mediated inward photocurrent in response to a 100-millisecond light pulse (620 nm, −60 mV holding potential). (B_2) Plot of ChrimsonR current amplitudes from 7 neurons (as B_1). (C) Optogenetic activation of ChrimsonR drives action potentials in POMC neurons: (C_1) 5 milliseconds at 5 Hz, (C_2) 20 milliseconds at 5 Hz, and (C_3) 5 milliseconds at 20 Hz. NTS, nucleus of the solitary tract; POMC, pro-opiomelanocortin.

Copyright © 2022 by the International Association for the Study of Pain. Unauthorized reproduction of this article is prohibited.

Instantaneous heart rate was monitored using a window discriminator to trigger off the R wave of the ECG signal. All signals were acquired with an analogue to digital converter (micro1401; CED, Cambridge, United Kingdom) to a computer running Spike2 software (CED). Intercostal EMG was extracted from the same recording by rectifying the signal and applying a median filter (time constant 60 ms) in Spike2 to monitor respiratory pattern.

For these acute optogenetic experiments, a 200-μm optic fibre (Lambda-B fibre, emitting length 2 mm + implant length 17 mm; Optogenix) connected to 550 nm LED (Lime PlexBright module, Plexon) was inserted 0.25 mm into the NTS from the surface of the medulla at the level of calamus scriptorius. The NTS was illuminated with 20-millisecond light pulses at 5 to 20 Hz for 5 seconds (2-3 minutes interval between consecutive stimulus trains). Three repetitions of each light train were applied at each frequency. The light intensity exiting the fibre was ~6 mW (measured before and after each experiment; Thorlabs power meter, PM400D). These were proof-of-concept experiments that informed the approach used for the optogenetic experiments in chronically implanted mice.

2.5.2. Chronic implanted optogenetic activation of NTS_{POMC} neurons

$NTS_{POMC(Chrim)}$ mice with a previously implanted optic fibre had ECG and intercostal muscle EMG recorded under light recovery anaesthesia using isoflurane (maintenance isoflurane 1%-1.5% in O_2). The anaesthetised mice were placed prone on a thermal heat pad. A wireless LED head-stage (Helios 620 nm; Plexon, Inc) was connected to the fibre optic. The light intensity exiting the fibre was ~2 mW (measured at implantation). The ECG/EMG recording arrangement was as for the acute ECG/EMG study (see 2.5.1) except that the signal was amplified and digitised using an INTAN head-stage (RHD2216), and the digitised signal was relayed via an acquisition system (Open-Ephys.org). The data were displayed and analysed in Spike2 and cardiorespiratory responses elicited using identical light stimulation parameters to those from the acute experiments. The involvement of endogenous opioids in the optogenetically evoked (20 ms × 20 Hz, 5 seconds) cardiorespiratory responses was assessed 30 minutes after injection of either the opioid antagonist naloxone (1 mg/kg, i.p.) or the 0.9% normal saline (NSS; i.p.). The experimenter was masked to drug identity with testing on different days (counterbalanced design). The experiment was also conducted in control implanted $NTS_{POMC(Gq)}$ mice (n = 4) to test whether an identical pattern of light stimulation alters cardiorespiratory function in mice without ChrimsonR expression.

2.5.3. Analysis of electroardiogram and electromyogram data

Instantaneous heart rate was calculated from the reciprocal of the R-R interval of ECG. The interbreath interval was calculated from onset of bursts in the intercostal EMG. To analyse the effect of opto-stimulation, the recording was divided into 4 phases: prebasal (*P*, 10 seconds), baseline (*B*, 10 seconds), during opto-stimulation (*O*, 5 seconds), and recovery (*R*, 10 seconds) (shown in Supplemental Figure 1, available at http://links.lww.com/PAIN/B733). The degree of bradycardia (%) was calculated (taking account of the spontaneous variation in heart rate and respiration within each of these periods) from the heart rate (HR) using the following formulae:

$$\text{Baseline bradycardia}(\%) = (\text{mean } P\text{–minimum B})/\text{mean } P \times 100$$

$$\text{Opto – stimulation bradycardia}(\%) = (\text{mean } P\text{–minimum O})/\text{mean } P \times 100$$

$$\text{Recovery bradycardia}(\%) = (\text{mean } P\text{–minimum R})/\text{mean } P \times 100.$$

Similarly, the degree of bradypnoea (%) was calculated from the maximum interbreath intervals using the following formulae:

$$\text{Baseline bradypnoea}(\%) = (\text{maximum } B\text{–mean P})/\text{mean } P \times 100$$

$$\text{Opto – stimulation bradypnoea}(\%) = (\text{maximum } O\text{–mean P})/\text{mean } P \times 100$$

$$\text{Recovery bradypnoea}(\%) = (\text{maximum } R\text{–mean P})/\text{mean } P \times 100.$$

To derive the opto-stimulation Δbradycardia (%), the baseline bradycardia (%) was subtracted from the opto-stimulation bradycardia (%). Similarly, Δbradypnoea (%) was derived from the difference between baseline bradypnoea (%) and opto-stimulation bradypnoea (%).

2.6. Acute pain assays

2.6.1. Hargreaves' test

Hargreaves' test was conducted to assess the degree and time course of analgesia.[21] In this test, a beam of infrared light (Harvard Apparatus) was directed onto the plantar surface of the hind paw and the withdrawal latency was recorded. A fixed intensity of illumination that produced a withdrawal latency between 3 and 5 seconds (for optogenetics and excitatory chemogenetics) or 5 to 7 seconds (for inhibitory chemogenetics) under baseline conditions was determined before the test session and used throughout the experiments. A maximum cut-off latency of 15 seconds for the Hargreaves' test was used to avoid tissue injury. All mice were habituated to the test apparatus 3 days before the experiment.

Implanted $NTS_{POMC(Chrim)}$ mice received opto-stimulation using the wireless LED headset (20 ms pulses × 5 Hz, 1 minute) to assess the effect on thermal withdrawal. To establish the time course of any effect, the mice had a single period of opto-stimulation and the withdrawal latency was assessed over the next hour (at 5, 10, 20, 30, 40, 50, and 60 minutes). Each $NTS_{POMC(Chrim)}$ (n = 6) mouse was then tested for 3 consecutive days (randomly allocated, counterbalanced design) under 3 conditions: (1) baseline (without opto-stimulation); (2) opto-stimulation (20 ms pulses × 5 Hz, 1 minute) after 0.9% normal saline solution injection (NSS, i.p.); and (3) opto-stimulation after naloxone injection (1 mg/kg, i.p.). Four repeated measures were taken under each condition at intervals of 10 minutes. Naloxone/NSS was administered 15 minutes before the start of the first test. The experimenter was masked to drug (NSS/Naloxone). The same experimental protocol was repeated in control mice (implanted $NTS_{POMC(Gq)}$, n = 6) to assess the effect of light alone on withdrawal latency in the Hargreaves' test.

The Hargreaves' test was also conducted for chemogenetic studies in $NTS_{POMC(Gq)}$ (n = 6, excitatory) and $NTS_{POMC(Gi)}$ (n = 6, inhibitory) mice. On different days, the mice received either (1) NSS injection (i.p.) or (2) clozapine N-oxide dihydrochloride injection (3 mg/kg, i.p., subsequently abbreviated to CNO). The $NTS_{POMC(Gq)}$ mice also had a third condition with naloxone (1 mg/kg, i.p.) in addition to CNO injection. All drugs (NSS/CNO/Naloxone; i.p.) were administered 15 minutes before the start of the first Hargreaves' test, and 4 repeated measurements were taken in each animal at intervals of 10 minutes. The experimenter was masked to drug allocation and the allocation to drug was counterbalanced. The experiment was also repeated with CNO

Copyright © 2022 by the International Association for the Study of Pain. Unauthorized reproduction of this article is prohibited.

dosing to control mice ($NTS_{POMC(Chrim)}$, n = 6) to test whether CNO injection has an effect on withdrawal latency in Hargreaves' test.

2.6.2. Tail-flick test

The tail-flick test was conducted to assess the analgesic efficacy of activation of POMC neurons by both optogenetics and chemogenetics. The mouse was wrapped in a soft towel and 2 to 3 cm of its tail tip was dipped into water (45°C for optogenetic study and 50°C for chemogenetics) to assess the withdrawal latency. A cut-off of 20 seconds for the tail flick was used to avoid tissue injury. The experimental comparisons were similar to the Hargreaves' test. The mice were habituated for 2 days before the test protocol. The experiment was also repeated in control vector–injected mice (implanted $NTS_{POMC(Gq)}$, n = 6 for optogenetics and $NTS_{POMC(Chrim)}$, n = 6 for chemogenetics).

2.7. Conditioned place preference testing

Condition place preference (CPP) test was conducted in the $NTS_{POMC(Chrim)}$ (n = 6) and $NTS_{POMC(Gq)}$ (n = 6) mice to assess whether optogenetic or chemogenetic activation of NTS_{POMC} neurons, respectively, produces preference or aversion. The CPP testing apparatus consists of 2 distinct chambers (each 190 × 230 mm, one with horizontal black and white striped walls and horizontal grating floor and the other with vertical black and white striped walls and perforated floor). The chambers were joined by a clear plastic external corridor. Each animal was habituated for 15 minutes the day before the start of the conditioning protocol where the animal was allowed to freely explore both the chambers of the CPP box.

Each $NTS_{POMC(Chrim)}$ mouse was conditioned for 2 consecutive days (morning/afternoon) with opto-stimulation (20 ms pulses at 5 Hz for 5 minutes) in one of the CPP arena chambers (counterbalanced design). On the alternate session (morning/afternoon) of these 2 days, the test animal was also allowed to freely explore the other chamber (nonconditioned) for 5 minutes with its head-stage attached. On the test day, the animal was placed inside the common external corridor between the 2 chambers (with the wireless LED head-stage attached) and allowed to freely explore the 2 chambers for 15 minutes.

For the chemogenetic experiments, each $NTS_{POMC(Gq)}$ mouse was allowed to spend 15 min/day either in the conditioned (CNO, 3 mg/kg, i.p., alternate days) or in the nonconditioned (NSS, i.p., alternate days) CPP chamber for 4 days. During this conditioning phase, the animals were dosed with CNO/NSS and then returned to their home cage for 15 minutes before being put in the CPP chamber. On the test day, the animal was placed inside the common external corridor between the 2 chambers and allowed to freely explore the 2 chambers for 15 minutes.

The experiments were video-recorded, and the video files were coded allowing blinding before analysis. The time spent in each chamber before (15 minutes habituation period) and after conditioning (15 minutes test period) was analysed (Ethovision, Noldus, the Netherlands). The proportion of time spent by the animals between conditioned and unconditioned chamber was compared. Additionally, the percentage of time spent in the conditioned chamber by each animal before and after conditioning was also contrasted.

2.8. Open field test

Open field testing was conducted to determine whether chemogenetic activation of NTS_{POMC} neurons caused any anxiolytic changes in behaviour or locomotor activity in the $NTS_{POMC(Gq)}$ mice (n = 5). In this test, 15 minutes after the injection of CNO (3 mg/kg, i.p.), the mouse was placed in an open field box (50 × 50 cm) and allowed to freely move around the arena for 15 minutes. The experiment was also conducted in control mice ($NTS_{POMC(Chrim)}$, n = 4) using the same protocol for comparisons. The test was video recorded and blinded off-line analysis was done to evaluate the time spent in the central arena and the total distance moved by the experimental vs control mice.

2.9. Persistent pain models

2.9.1. Tibial nerve transection

To produce a neuropathic pain model, mice underwent surgery for tibial nerve transection (TNT), a model that has shown to induce robust and long-lasting hypersensitivity.[23,24,31,45] Mice were anaesthetized with isoflurane (5% in O_2 until loss of consciousness and maintained at 1%-2% isoflurane in O_2). A 5-mm incision was made through the skin over the right thigh parallel to the femur and the sciatic nerve was exposed, allowing identification of the tibial nerve. The isolated tibial nerve branch was ligated with 6-0 silk thread as distally as possible. Three millimeters of the nerve proximal to the ligation was transected and removed, and the ligature was left in place. The skin was sutured with 6-0 silk thread, and the animals were left to recover for 1 week. Sensory testing with acetone (cold sensitivity) and von Frey filaments (punctate pressure sensitivity) was performed before surgery and again 2 to 3 weeks after nerve transection after administration of CNO/NSS.

2.9.2. Carrageenan inflammatory pain model

Inflammatory sensitisation was induced by injecting the plant-derived mucopolysaccharide, λ-carrageenan, following the protocol of McCarson et al.[34] Mice were briefly anaesthetised with isoflurane, and the right hind paw was disinfected with 70% ethanol and iodine solution. Then 25 μL of 0.5% λ-carrageenan (Merck, dissolved in sterile dH_2O) was injected (25-gauge syringe needle) in the right hind paw foot pad. Mice were returned to their cage and developed sensitisation and oedema after approximately 3.5 hours, which lasted until the end of the experiment (8 hours). Sensory testing (von Frey) was conducted 15 minutes after administration of NSS/CNO (administered sequentially with >1 hour between i.p. injections, at 3.5 and 5 hours after carrageenan, respectively). A subsequent set of tests was conducted 2.5 hours post-CNO injection to assess whether any effect of chemoactivation resolves by this time point.

2.9.3. Punctate mechanical—von Frey test

To assess the degree of mechanical hyperalgesia, animals that underwent either tibial nerve transection (n = 6) or carrageenan injection (n = 4) were tested by applying von Frey filaments of varying force in the mid-lateral plantar area of the right hind paw, to identify the threshold that produces a withdrawal. The starting filament applied was 1*g* (4.08). The 50% withdrawal threshold was identified using the up and down method [14] and is reported in grams.

2.9.4. Cold sensitivity—acetone test

To identify the presence of cold allodynia in TNT mice (n = 6), a drop of acetone was applied to the mid-lateral plantar area of the

Copyright © 2022 by the International Association for the Study of Pain. Unauthorized reproduction of this article is prohibited.

right hind paw and the nocifensive events (paw raises, licking, and shaking) were scored over 60 seconds. The test was repeated 3 times 5 minutes apart and the mean value is reported.

2.10. Spirometry

To assess whether activation of NTS_{POMC} neurons produces respiratory depression in freely behaving mice, spirometry was conducted in plethysmography chambers (EMKA Technologies, Paris, France), supplied with room air and with differential pressure transducers connected to a computer. All mice were habituated to the apparatus for 30 minutes the day before the experiment. The experiment was conducted on 2 consecutive days where each mouse ($NTS_{POMC(PSAM)}$ or $NTS_{POMC(Gq)}$), respectively, received either chemogenetic agonist ($PSEM^{89s}$ 90 mg/kg) or CNO (3 mg/kg, i.p.) compared with control NSS (i.p.) (counterbalanced design). The minute volume was recorded in the plethysmograph for 60 minutes under each condition. A 15-minute baseline recording was taken before the start of the experiment. The experiment was also conducted in control mice ($NTS_{POMC(Chrim)}$, n = 2) using the same test protocol. Drug administration was randomised, and the experimenter was blinded to the treatment.

Initial experiments using the PSAM strategy (Cerritelli et al. 2016) showed evidence for a significant depression of respiration with $PSEM^{89s}$ when compared with NSS (Supplemental Figure 2, available at http://links.lww.com/PAIN/B733) but a similar degree of respiratory depression was observed in control mice, suggesting that this dose of $PSEM^{89s}$ had off-target effects on respiratory control and so all subsequent experiments used the DREADD hM3Dq chemogenetic strategy.

2.11. Stress-induced analgesia

A 3-minute swim in 32°C water[15,47] was used to generate stress-induced analgesia. This was assessed with tail-flick assay performed before and 1 minute after the swim. For the tail-flick assay, the mouse was dried and wrapped with a soft towel, and the distal third of its tail was dipped into 50°C water to measure the tail withdrawal latency. Both the $NTS_{POMC(Gi)}$ (n = 8)/$ARC_{POMC(Gi)}$ (n = 3) and the control ($NTS_{POMC(Chrim)}$, n = 6) mice were injected with either CNO or NSS 15 minutes before the swim, which was repeated on consecutive days (counterbalanced design, experimenter blinded to drug). Two repeat measurements (at 1 minute interval) were taken at each time point to obtain the average tail withdrawal latency.

2.12. Histology

All mice were euthanised (pentobarbital sodium 100 mg/kg, i.p.) at the end of study, and brains were fixed by cardiac perfusion with 10% formalin. After fixation, the brains were postfixed in 10% formalin for a day and then cryopreserved in 30% sucrose at 4°C. Coronal slices (50 μm) were cut on a freezing microtome and then mounted and observed on an epifluorescent microscope (Leica DM4000B; Leica Microsystems, Wetzlar, Germany, GmbH) to confirm the expression of ChrimsonR-tdTomato/hM3Dq-mCherry/hM4Di-mCherry in the NTS/ARC. Animals that had failed virus transduction were excluded from the group and used as internal experimental controls as appropriate.

2.13. Statistical analysis

Statistical analysis was conducted using GraphPad Prism 7 (GraphPad Software, Inc., San Diego, CA). Technical replicates obtained from each animal were averaged first before performing analysis. The statistical tests used for analysis are reported in the respective result sections. Results were reported as mean ± SEM or median (IQR), as appropriate. Differences were considered significant at $P < 0.05$, and experimental group sizes were based on the effect sizes from our previous study.[13] Where previous experimental data were not available, then an initial pilot was conducted with n = 3 animals to get an estimate of effect size and a power calculation was performed (beta < 0.1 and alpha < 0.05) to calculate the required group size. In most cases (unless otherwise specified), comparisons were made within animal (before vs after treatment). Experiments on control animals were done using the same testing protocol to demonstrate that observed effect was because of the optogenetic/chemogenetic modulation of the POMC neurons.

2.14. Materials

Naloxone hydrochloride (made to a stock solution of 10 mg/mL in dH_2O) and CNO dihydrochloride were from Tocris (Bristol, United Kingdom). All other salts and drugs were from Sigma, unless otherwise stated.

3. Results

3.1. Opto-stimulation of NTS_{POMC} neurons in brain slices

To enable opto-stimulation of NTS_{POMC} neurons, we aimed to express ChrimsonR that has the potential advantage in vivo of relatively large photocurrents and has a red shifted excitation spectrum that allows better light penetration in brain tissue.[29] To confirm the efficacy of optoexcitation, whole-cell recordings were made from NTS_{POMC} neurons transduced with ChrimsonR, identified by tdTomato fluorescence, in acute slices of medulla (**Fig. 1A**, n = 7). All the $tdTomato^+$ neurons showed time-locked inward currents in response to pulses of illumination (610 nm, 5-100 ms; voltage clamped at $V_h = -60$ mV) with a mean inward current of 248 ± 114 pA (**Fig. 1B**, n = 7). Current clamp recordings of the same $NTS_{POMC(Chrim)}$ neurons showed that opto-stimulation could reliably drive action potentials with a 1:1 ratio in neurons with either 5- or 20-millisecond pulses at frequencies between 1 and 20 Hz (**Fig. 1C**).

3.2. High-frequency opto-stimulation of NTS_{POMC} neurons in anaesthetised mice evokes transient bradycardia and bradypnoea

As a proof-of-concept experiment, we assessed whether opto-stimulation of NTS_{POMC} neurons transduced with ChrimsonR produced changes in heart rate and respiration in vivo analogous to the effects seen in situ in the working heart–brainstem preparation.[13] An acutely placed fibre-optic probe was lowered into the NTS of isoflurane anaesthetised mice (n = 3, Supplemental Figure 1, available at http://links.lww.com/PAIN/B733). Opto-stimulation at 20 Hz induced a bradycardia (7.8% [1.7%-23.6%] vs baseline 0.06% [0.06%-0.4%]; $P = 0.03$, Friedman test with the Dunn post hoc test, but this was not seen at lower frequencies (2 Hz, $P = 0.22$ or 5 Hz, $P = 0.22$, Friedman test). The bradycardia produced by 20 Hz opto-stimulation was transient and returned to the baseline within 10 seconds (recovery 1.0% [0.6%-3.4%] vs baseline; Dunn post hoc test, $P = 0.44$.

This opto-stimulation of NTS_{POMC} neurons simultaneously produced a graded bradypnoea with an increased interbreath interval at 20 Hz (213% [172%-545%] vs baseline 8.2% [8.1%-

Copyright © 2022 by the International Association for the Study of Pain. Unauthorized reproduction of this article is prohibited.

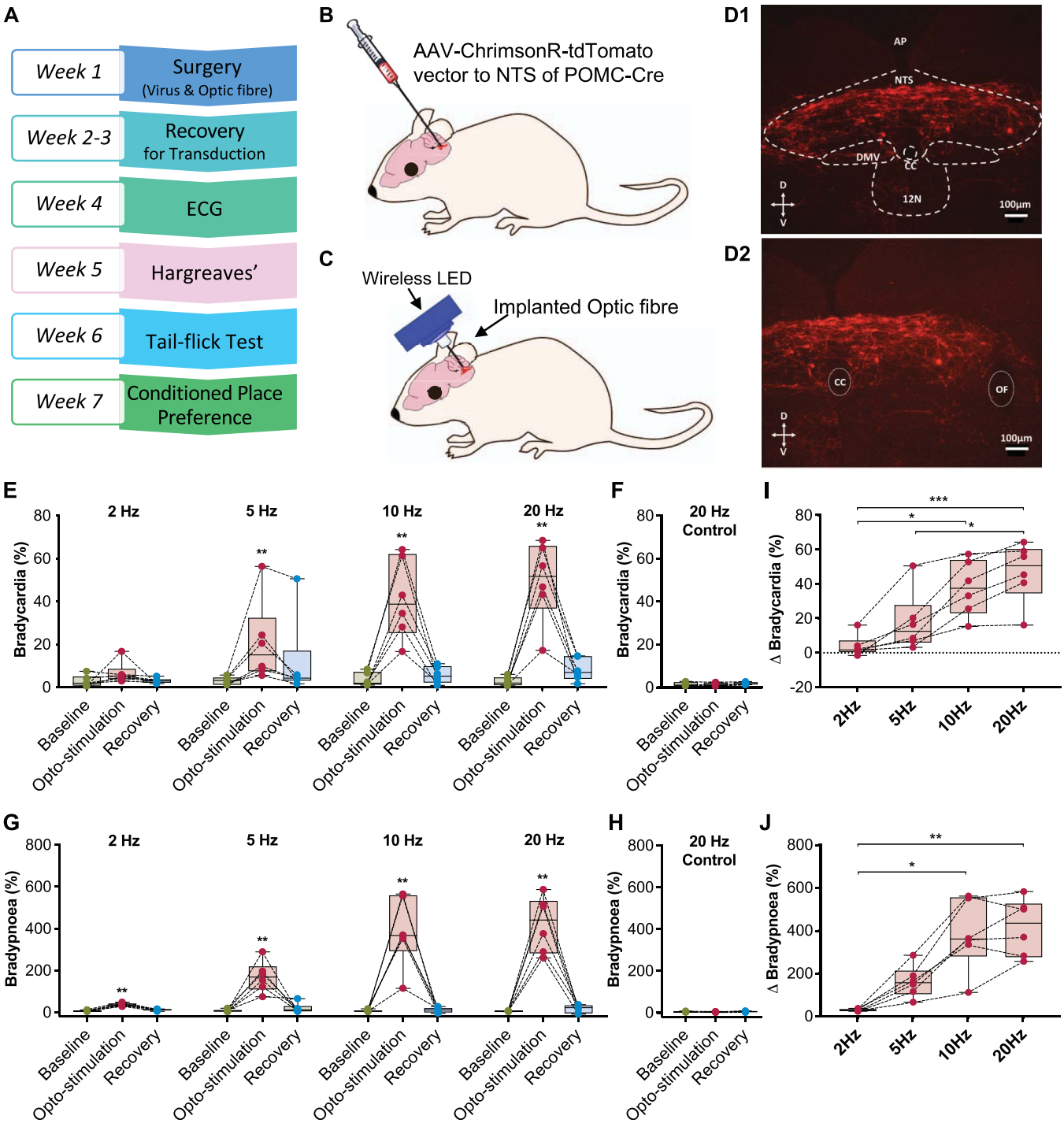


Figure 2. Cardiorespiratory effect of opto-stimulation of NTS_{POMC} neurons in chronically implanted mice (A). Timeline for optogenetic experiments in implanted mice (pain tests and CPP data shown in Fig. 3). (B) Injection of AAV-ChrimsonR-tdTomato into the NTS of POMC-Cre mice (C). Schematic diagram shows opto-stimulation of NTS_{POMC} neurons via wireless LED attached to optic fibre (20 ms × 5-20 Hz, 5 seconds). Representative histological section of brain stem shows (D1). NTS_{POMC} neurons expressing tdTomato (D2). Optic fibre location (OF) in the NTS in ChrimsonR-tdTomato–injected mice (E). Opto-stimulation in $NTS_{POMC(Chrim)}$ mice (n = 6) produced bradycardia at 5 Hz (15.2% vs 3.2%), 10 Hz (38.7% vs 1.9%), and 20 Hz (51.7% vs 1.9%) compared with baseline. Heart rate returned to baseline values during recovery period (within 10 seconds) (F). Opto-stimulation produced no bradycardia in control implanted $NTS_{POMC(Dq)}$ mice (n = 4). (G) Opto-stimulation at all frequencies (2-20 Hz) in NTS_{POMC}(Chrim) mice (n = 6) produced bradypnoea (35.9% vs 7.4%, 168.9% vs 7%, 367.1% vs 5.5%, 440.7% vs 6.2%, respectively) compared with baseline values. The respiratory rate returned to baseline values within 10 seconds of the end of illumination. (H) Opto-stimulation did not affect respiratory rate in control $NTS_{POMC(Dq)}$ mice (n = 4) (I and J). The Δbradycardia and Δbradypnoea in $NTS_{POMC(Chrim)}$ mice (n = 6) were dependent on opto-stimulation frequency. Data presented as median, min to max and analysed by Friedman test with Dunn post hoc test. $^{*}P < 0.05$, $^{**}P < 0.01$, $^{***}P < 0.001$. AAV, adeno-associated viral vector; CPP, condition place preference; LED, light emitting diode; NTS, nucleus of the solitary tract; POMC, pro-opiomelanocortin.

Copyright © 2022 by the International Association for the Study of Pain. Unauthorized reproduction of this article is prohibited.

9.5%]; $P = 0.03$) and 10 Hz (81% [53%-231%] vs baseline 14% [8.6%-16%]; $P = 0.03$, Friedman test with Dunn post hoc test) but not at 5 Hz (53% [18%-62%] vs baseline 8.9% [7.9%-10.9%]; $P = 0.2$; Supplemental Figure 1F, available at http://links.lww.com/PAIN/B733). As with the bradycardia, these respiratory pauses were short-lived and recovered to baseline within 10 seconds of the end of opto-stimulation (Dunn post hoc test, $P = 0.44$).

The cardiorespiratory depressant effects were specific to NTS_{POMC} neuronal activation as no effect was observed when the probe was placed lateral or rostral to the NTS. The patterns of bradycardia and bradypnoea were identical in character to those seen in the working heart–brainstem preparation in response to activation of NTS_{POMC} neurons,[13] which confirmed successful optogenetic targeting and activation of NTS_{POMC} neurons in vivo with ChrimsonR.

3.3. Opto-stimulation of NTS_{POMC} neurons in implanted mice produces a graded, transient bradycardia and bradypnoea

To allow longitudinal studies and combined assays of cardiorespiratory function and pain-related behaviours, $NTS_{POMC(Chrim)}$ mice (n = 6) were implanted chronically with an optic fibre (**Figs. 2A and D**). Recordings under isoflurane anaesthesia showed opto-stimulation produced graded transient bradycardia (**Fig. 2E** and Supplemental Figure 3, available at http://links.lww.com/PAIN/B733) with a reduction in heart rate at 5 to 20 Hz frequencies ($P < 0.01$, Friedman test with Dunn post hoc test) but not at 2 Hz (Friedman test, $P = 0.052$). An identical illumination protocol in implanted control $NTS_{POMC(Dq)}$ mice did not produce any effect on heart rate even at the maximum stimulus frequency (20 Hz, n = 4, **Fig. 2F**, Supplemental Figure 3E, available at http://links.lww.com/PAIN/B733). Opto-stimulation in $NTS_{POMC(Chrim)}$ mice (n = 6) also produced graded bradypnoea with an increase in interbreath interval at all frequencies ($P < 0.01$, Friedman test with Dunn post hoc test, **Fig. 2G** and Supplemental Figure 3, available at http://links.lww.com/PAIN/B733). Again, an equivalent illumination protocol in implanted $NTS_{POMC(Dq)}$ control mice had no effect on respiration (20 Hz, n = 4, **Fig. 2H**). Both the bradycardia and the bradypnoea were frequency dependent (Friedman test, $P < 0.0001$). The opto-stimulation–induced Δbradycardia was significantly larger at 10 Hz ($P = 0.04$) compared with 2 Hz and at 20 Hz compared with both 2 Hz ($P = 0.0003$) and 5 Hz (Dunn post hoc test, $P = 0.04$; **Fig. 2I**). Similarly, the Δbradypnoea was significantly larger at 10 Hz ($P = 0.01$) and 20 Hz ($P = 0.002$) compared with 2 Hz (**Fig. 2J**). The heart rate and respiratory rate rapidly recovered after illumination stopped (recovery vs baseline, $P > 0.05$).

3.4. NTS_{POMC} bradycardia is opioid mediated

Administration of the opioid antagonist naloxone (1 mg/kg, i.p.) 30 minutes before opto-stimulation (20 Hz) attenuated the NTS_{POMC}-evoked bradycardia (naloxone 31% [11%-59%] vs NSS 56% [38%-67%]; $P = 0.03$, Wilcoxon matched-pairs signed rank test, Supplemental Figure 4, available at http://links.lww.com/PAIN/B733) but not the bradypnoea (naloxone 203% [73%-314%] vs NSS 339% [163%-390%]; $P = 0.31$.

3.5. Opto-stimulation of NTS_{POMC} neurons produces sustained opioid-mediated analgesia

To investigate whether opto-stimulation of NTS_{POMC} neurons produces analgesia, the tail-flick assay was used. Based on the findings from the cardiorespiratory study above, we used a light stimulation paradigm that was the lowest frequency that produced consistent physiological effects (20 ms × 5 Hz). Such opto-stimulation in implanted $NTS_{POMC(Chrim)}$ mice increased the tail-flick latency (from 5.9 ± 0.3 seconds baseline to 18.8 ± 0.6 seconds, 1 way repeated measures analysis of variance [RM-ANOVA] with Tukey post hoc test, n = 6, $P < 0.0001$, **Fig. 3B**). This was attenuated by naloxone treatment (9.33 ± 0.85 s vs 18.8 ± 0.6 s NSS, $P = 0.0004$; 1 mg/kg, i.p. 15 minutes before test; **Fig. 3B**), but this did not completely return the latency to baseline (Tukey post hoc test, $P = 0.01$). Implanted control mice showed no change in their tail-flick latency after identical illumination (implanted $NTS_{POMC(Gq)}$, $P = 0.43$, paired t test, n = 6, **Fig. 3C**).

A similar analgesic action was also found in the Hargreaves test. NTS_{POMC} opto-stimulation (20 ms × 5 Hz, 1 minute) increased hind paw withdrawal latency (1-way RM-ANOVA, $P < 0.0001$, n = 6). This showed an increase in paw withdrawal latency after opto-stimulation (10.7 ± 0.9 seconds NSS vs 4.5 ± 0.8 seconds baseline, $P = 0.0005$, Tukey multiple comparison test, **Fig. 3D**). Naloxone attenuated the effect of NTS_{POMC} opto-stimulation on paw withdrawal latency (6.2 ± 0.5 seconds, Tukey post hoc test, $P = 0.002$; 1 mg/kg, i.p. injection 15 minutes before test; **Fig. 3D**) compared with NSS, but there was still a small increase in withdrawal latency compared with baseline (Tukey post hoc test, $P = 0.02$). No change in withdrawal latency was observed in implanted control mice after opto-stimulation (implanted $NTS_{POMC(Gq)}$, $P = 0.82$, paired t test, n = 6, **Fig. 3E**).

To determine the time course of analgesic effect, NTS_{POMC} neurons in the same implanted $NTS_{POMC(Chrim)}$ mice were optoactivated (for 1 minute at 5 Hz) and the hind paw withdrawal latency was assessed repeatedly using the Hargreaves test (**Fig. 3F**). The withdrawal latency showed a significant effect of time (1-way RM-ANOVA, $P < 0.0001$, n = 6). The withdrawal latency was prolonged during opto-stimulation (14.2 ± 0.5 seconds, $P < 0.001$) and it remained elevated for the following 30 minutes (5 minutes [9.5 ± 0.8 seconds, $P < 0.01$], 10 minutes [8.9 ± 0.7 seconds, $P < 0.001$], 20 minutes [8.2 ± 0.7 seconds, $P < 0.001$], and 30 minutes [6.9 ± 0.8 seconds, $P < 0.01$]) compared with baseline (4.9 ± 0.7 seconds).

3.6. Opto-stimulation of NTS_{POMC} neurons does not produce preference/aversion

Given that the naloxone blockade of the analgesic effects suggested the release of β-endorphin from NTS_{POMC} neurons, we sought to identify whether this had an affective valence in the CPP test. No difference was observed in the time spent by these implanted $NTS_{POMC(Chrim)}$ mice between the opto-stimulation conditioned vs unconditioned chamber (52.6 ± 5.1% vs 47.4 ± 5.1%, respectively, n = 6, $P = 0.49$, Welch t test; **Fig. 3G**). Furthermore, the time spent in the conditioned chamber before (15 minutes habituation period) and after conditioning (15 minutes test period) was also unchanged (51.6 ± 3.1 vs 52.6 ± 5.1%, n = 6, $P = 0.87$, Welch t test, **Fig. 3H**).

3.7. Chemogenetic activation of NTS_{POMC} neurons produces analgesia

The synchronous optoactivation of NTS_{POMC} neurons is likely to be a nonphysiological pattern of activity, and therefore, we extended our study to assess whether DREADD chemogenetic activation of NTS_{POMC} neurons (CNO, 3 mg/kg, i.p., **Figs. 4A–C**), which may be considered as augmenting the ongoing activity in the circuit, also produced analgesia in the tail-flick and Hargreaves assays. In the tail-

Copyright © 2022 by the International Association for the Study of Pain. Unauthorized reproduction of this article is prohibited.

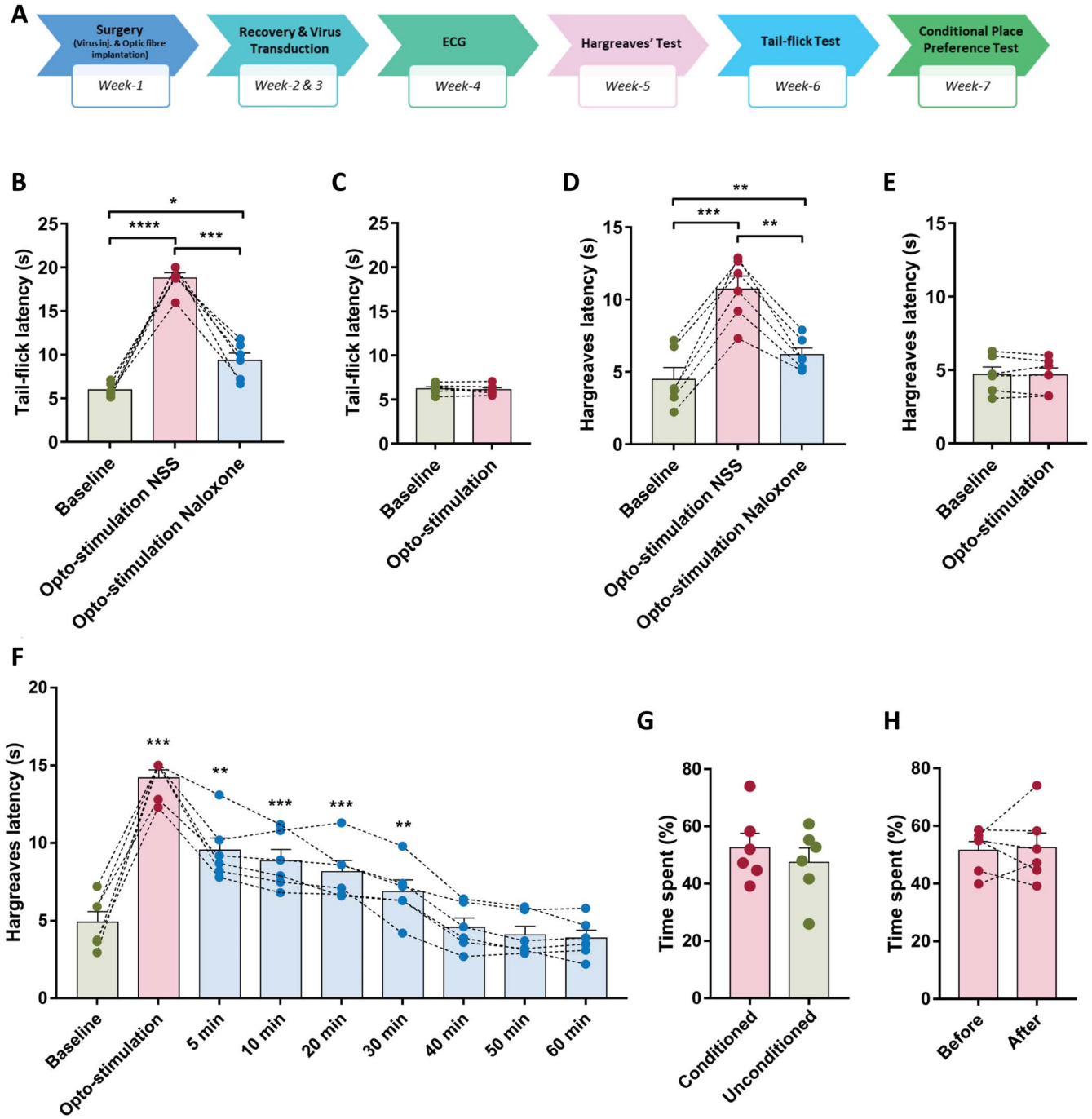


Figure 3. Effect of opto-stimulation of NTS_{POMC} neurons on analgesia and preference/avoidance. (A) Timeline for optogenetic experiments in implanted $NTS_{POMC(Chrim)}$ mice. Opto-stimulation of NTS_{POMC} neurons (20 ms pulse at 5 Hz for 1 minute) produced increased withdrawal latency in both the tail-flick test (B) and the Hargreaves test (D), which was reduced by opioid antagonist naloxone (n = 6, 1-way RM-ANOVA with Tukey post hoc test). Identical opto-stimulation in implanted control vector–injected mice had no effect on latencies in either the tail-flick test (C) or the Hargreaves test (E) (n = 6, paired *t* test). (F) Time course of analgesia assessed in Hargreaves' test. A sustained analgesia was observed until 30 minutes post-activation of these neurons (n = 6, 1-way RM-ANOVA with Tukey's post-hoc test). (G) Conditioned place preference testing showed that opto-stimulation in $NTS_{POMC(Chrim)}$ mice had no significant effect on the time spent in opto-stimulation conditioned vs unconditioned chamber (assessed after conditioning, n = 6, Welch *t* test) or (H) on the time spent before (15 minutes habituation period) vs after conditioning (15 minutes test period) in conditioned chamber (paired *t* test). Data are presented as mean ± SE. $^{*}P < 0.05$, $^{**}P < 0.01$, $^{***}P < 0.001$, $^{****}P < 0.0001$. ANOVA, analysis of variance; NSS, normal saline solution; NTS, nucleus of the solitary tract; POMC, pro-opiomelanocortin.

flick assay, CNO administration increased withdrawal latency in $NTS_{POMC(Gq)}$ mice (CNO 3.1 ± 0.25 seconds vs NSS 1.9 ± 0.22 seconds, n = 6, $P < 0.05$, 1-way RM-ANOVA with Tukey post hoc test, **Fig. 4D**). Naloxone treatment (1 mg/kg, i.p.) attenuated the analgesia produced by NTS_{POMC} chemoactivation (CNO + naloxone withdrawal latency 2.3 ± 0.18 seconds, n = 6, $P < 0.01$ vs CNO, **Fig. 4D**) to a level comparable with baseline ($P = 0.17$, Tukey post hoc test). In contrast, administration of CNO to control mice ($NTS_{POMC(Chrim)}$) had no effect on withdrawal latency in tail-flick assay (n = 6, $P = 0.75$, paired *t* test, **Fig. 4E**).

Similar analgesia was seen in the Hargreaves test with chemo-activation prolonging latency to paw withdrawal in $NTS_{POMC(Gq)}$ mice (CNO 5.7 ± 0.43 seconds vs NSS 2.6 ± 0.25 seconds, n = 6, $P < 0.01$, 1-way RM-ANOVA with Tukey post hoc test, **Fig. 4F**).

Copyright © 2022 by the International Association for the Study of Pain. Unauthorized reproduction of this article is prohibited.

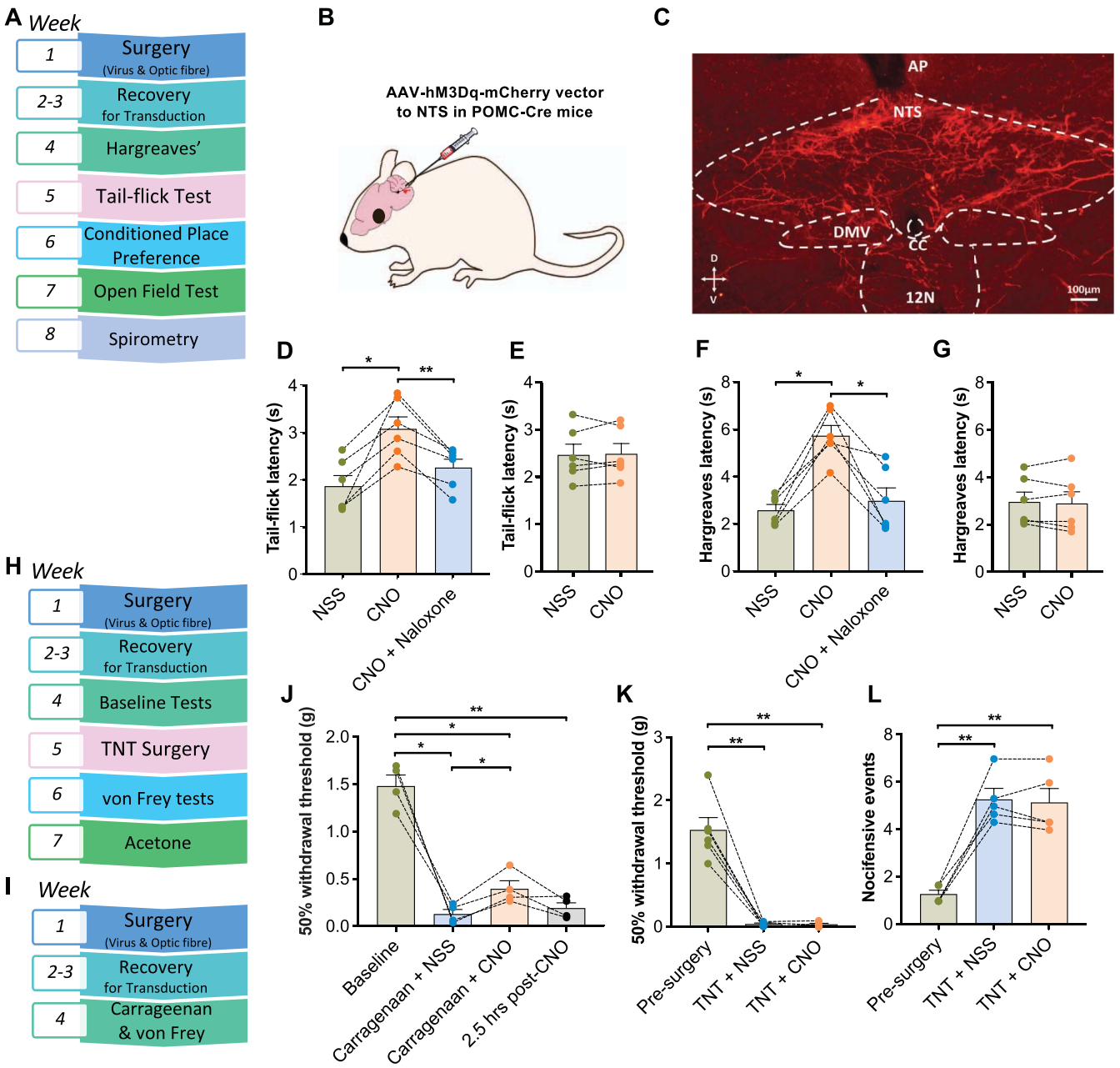


Figure 4. Chemogenetic activation of NTS_{POMC} neurons is analgesic in acute thermal and inflammatory pain models but not in a neuropathic model. (A) Timeline for acute chemogenetic experiments. (B) Schematic diagram shows injection of AAV-hM3Dq-mcherry into the NTS of POMC-Cre mice. (C) Representative histological section of brain stem shows NTS_{POMC} neurons expressing mCherry in $NTS_{POMC(Gq)}$ mice. Chemogenetic activation in $NTS_{POMC(Gq)}$ mice with CNO (3 mg/kg, i.p.) produced increased (D) tail flick and (F) paw withdrawal latencies, respectively, which were blocked by the opioid antagonist naloxone (1 mg/kg, i.p.) (n = 6, 1-way RM-ANOVA with Tukey post hoc test). In contrast, CNO showed no effect in control $NTS_{POMC(Chrim)}$ mice in the (E) tail-flick test (n = 6) or (G) Hargreaves test (n = 6) (paired *t* test). (H) Timeline for carrageenan-induced inflammatory pain experiment. (I) Timeline for TNT-induced neuropathic pain experiment. (J) Hind paw injection of carrageenan produced mechanical allodynia that was evident with control NSS injection (von Frey, 3.5 hours after carrageenan). Chemoactivation of the NTS_{POMC} neurons (CNO 3 mg/kg, i.p., 5 hours after carrageenan) significantly increased the paw withdrawal threshold (n = 5, $P < 0.05$, 1-way RM-ANOVA with Tukey post hoc test). The sensitisation returned on retesting 2.5 hours after CNO. (K) After TNT surgery, the $NTS_{POMC(Gq)}$ mice exhibit mechanical allodynia (von Frey assessed after 3 weeks) but subsequent CNO injection (3 mg/kg, i.p.) has no effect on paw withdrawal threshold (n = 6, $P > 0.05$, 1-way RM-ANOVA with Tukey post hoc test). (L) Acetone testing showed cold allodynia in $NTS_{POMC(Gq)}$ TNT mice with an increase in the number of nocifensive responses in 1 minute (tested 2 weeks after TNT). Again, CNO injection (3 mg/kg, i.p.) had no effect on acetone-evoked nocifensive responses (n = 5, $P > 0.05$, 1-way RM-ANOVA with Tukey post hoc test). For (K) and (L), CNO or NSS was administered on consecutive days (counterbalanced design and experimenter blinded to drug). Each value is an average of 3 measures. In each trial, testing was done 15 minutes after injection of CNO/NSS. Data are presented as mean ± SE. $^{*}P < 0.05$, $^{**}P < 0.01$, $^{***}P < 0.001$. RM-ANOVA, analysis of variance; AAV, adeno-associated viral vectors; NSS, normal saline solution; NTS, nucleus of the solitary tract; POMC, pro-opiomelanocortin; TNT, tibial nerve transection; DMV, Dorsal Vagal Motor Nucleus; AP Area Postrema; CC, central canal; 12N, hypoglossal.

Copyright © 2022 by the International Association for the Study of Pain. Unauthorized reproduction of this article is prohibited.

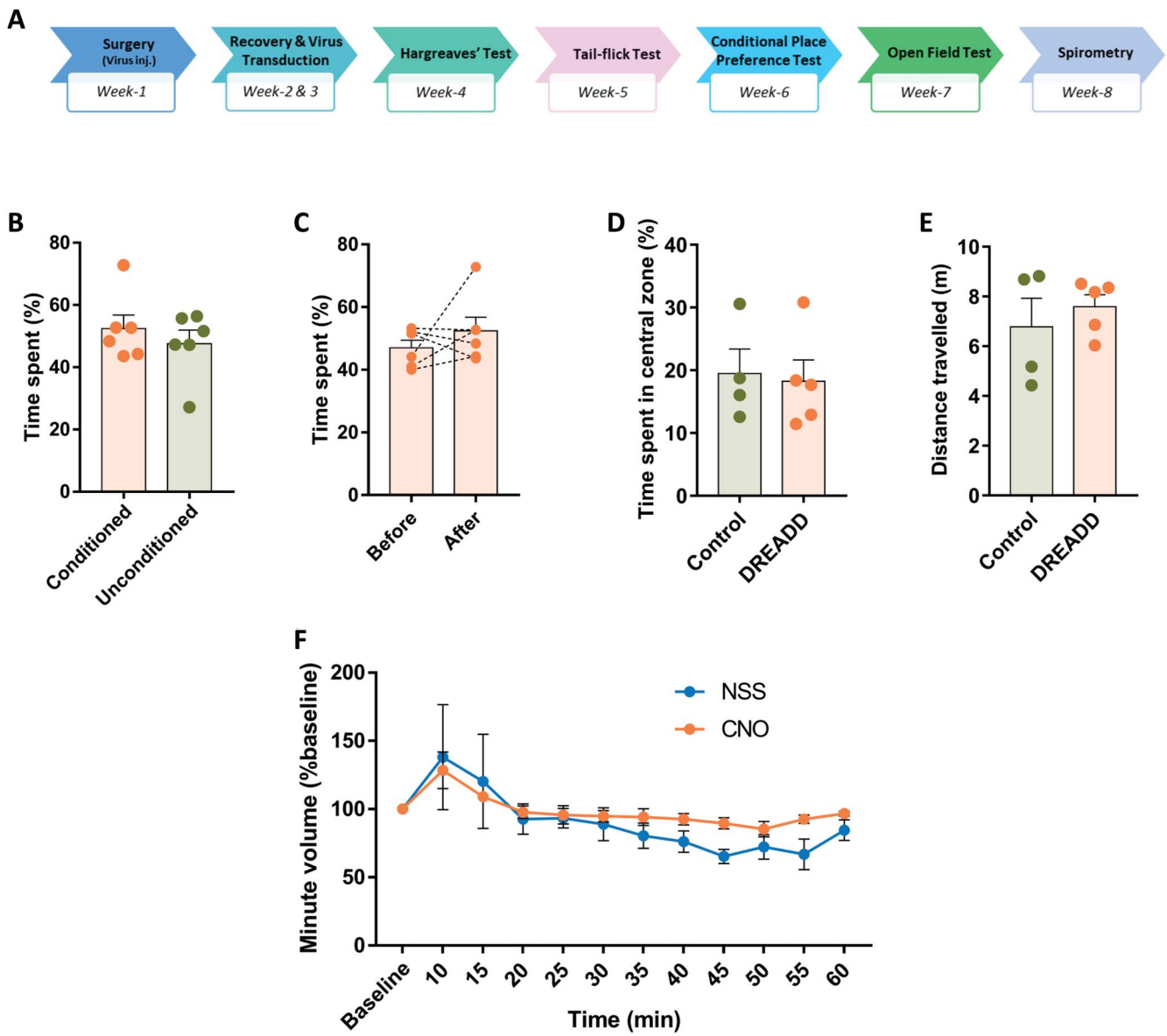


Figure 5. Chemoactivation of NTS_{POMC} neurons has no aversive, anxiogenic, locomotor, or respiratory depressant actions. (A) Timeline for chemogenetic experiments. The affective valence of chemogenetic activation of NTS_{POMC} neurons was assessed in a conditioned place preference test that showed no difference in either (B) proportion of time spent in CNO conditioned vs unconditioned chamber (n = 6, Welch's *t* test) or (C) percentage of time spent in CNO chamber before vs after the conditioning (paired *t* test). To identify any change in anxiety-like behaviour, the $NTS_{POMC(Gq)}$ mice were tested in an open-field arena. (D) No difference was observed in the time spent in the central zone of the arena by $NTS_{POMC(Gq)}$ mice (n = 5) compared with control $NTS_{POMC(Chrim)}$ mice (n = 4) after CNO (3 mg/kg, i.p., $P > 0.05$, Welch *t* test). (E) No change was observed in the distance travelled by the $NTS_{POMC(Gq)}$ mice compared with control mice after CNO injection (3 mg/kg, i.p., $P > 0.05$, Welch *t* test). To test for respiratory depression associated with chemogenetic activation of NTS_{POMC} neurons, the animals had whole-body plethysmography (F). No difference was observed in minute volume (% baseline) of the $NTS_{POMC(Gq)}$ animals after CNO (3 mg/kg, i.p.) compared with NSS (n = 5, $P > 0.05$, 2-way RM-ANOVA Data are presented as mean ± SE. $^{*}P < 0.05$, $^{**}P < 0.01$. RM-ANOVA, analysis of variance; NSS, normal saline solution; NTS, nucleus of the solitary tract; POMC, pro-opiomelanocortin.

Naloxone treatment reduced the analgesia produced by NTS_{POMC} chemoactivation (3.0 ± 0.55 seconds, $P < 0.05$, Tukey post hoc test, **Fig. 4F**) to a latency comparable with baseline ($P = 0.48$, Tukey post hoc test). CNO administration to control mice ($NTS_{POMC(Chrim)}$) did not alter the withdrawal latency in Hargreaves test (n = 6, $P = 0.18$, paired *t* test, **Fig. 4G**).

We next assessed whether chemogenetic activation of NTS_{POMC} neurons could ameliorate neuropathic or carrageenan-induced inflammatory pain behaviour (**Figs. 4H and I**). Injection of carrageenan to the hind paw produced mechanical allodynia (von Frey) that developed over 3 hours (withdrawal force reduced to 0.13 ± 0.05*g* from baseline 1.48 ± 0.12*g*, $P < 0.05$, 1-way RM-ANOVA with Tukey post hoc test, **Fig. 4J**). CNO administration to $NTS_{POMC(Gq)}$ carrageenan mice attenuated the mechanical hypersensitivity (0.40 ± 0.09*g*, $P < 0.05$, Tukey post hoc test). This analgesic effect diminished over a period of 3 hours to be statistically indistinguishable from the level of sensitisation pre-CNO injection (0.19 ± 0.06*g*, Tukey post hoc test, **Fig. 4J**). After TNT surgery, mice exhibited mechanical (von Frey) and cold (acetone) allodynia when tested 2 to 3 weeks after nerve transection ($P < 0.01$, 1-way RM-ANOVA with Tukey post hoc test, **Figs. 4K and L**). Administration of CNO to $NTS_{POMC(Gq)}$ TNT mice did not alter mechanical or cold allodynia ($P > 0.05$, Tukey post hoc test).

Copyright © 2022 by the International Association for the Study of Pain. Unauthorized reproduction of this article is prohibited.

3.8. Chemogenetic activation of NTS_{POMC} neurons does not produce aversion/preference

Given that we had observed that naloxone attenuated the analgesic effect of chemogenetic activation of NTS_{POMC} neurons (Section 3.7) suggesting the release of β-endorphin, therefore we tested for an affective valence. In CPP testing, no significant difference was observed in the proportion of time spent in the CNO conditioned vs unconditioned chamber by the $NTS_{POMC(Gq)}$ animals (52.4 ± 4.4 vs 47.6 ± 4.4%, n = 6, $P = 0.45$, Welch *t* test, **Figs. 5A and B**). Moreover, the time spent in the conditioned chamber remained same before (during the 15 minutes of habituation period) and after conditioning (47.0 ± 2.4 vs 52.4 ± 4.4%, $P = 0.31$, Welch *t* test, **Fig. 5C**).

3.9. Chemogenetic activation of NTS_{POMC} neurons is not anxiolytic

To assess the effect of stimulation of NTS_{POMC} neurons on locomotion and anxiety-like behaviour, we conducted an open field test. The $NTS_{POMC(Gq)}$ animals (n = 5) spent similar time in the central arena compared with control animals ($NTS_{POMC(Chrim)}$, n = 4) after CNO injection ($P = 0.82$, Welch *t* test, **Fig. 5D**). There was no difference between the groups in the distance travelled during the test ($P = 0.55$, Welch *t* test, **Fig. 5E**).

3.10. DREADD-mediated chemogenetic activation of NTS_{POMC} neurons does not cause respiratory depression

Synchronous optogenetic activation of NTS_{POMC} neurons produced respiratory pauses. We also found chemogenetic activation with PSAM produced respiratory depression (although as previously noted this was likely because of an off-target action of the $PSEM^{89s}$ agonist alone, Supplemental Figure 2, available at http://links.lww.com/PAIN/B733). Therefore, spirometry was conducted in a plethysmography chamber to assess the effect of chemoactivation of NTS_{POMC} neurons upon respiration over a period of 1 hour after CNO (**Fig. 5F**). No change in minute volume (% baseline) was observed after activation of NTS_{POMC} in comparison with NSS injection (n = 5, $P = 0.94$, 2-way RM-ANOVA). Control mice did not show any change in minute volume with CNO dosing ($NTS_{POMC(Chrim)}$, n = 2, $P = 0.97$).

3.11. Chemogenetic inhibition of NTS_{POMC} neurons suppresses stress-induced analgesia

Next, we explored the role of NTS_{POMC} neurons in stress-induced analgesia using an inhibitory chemogenetic strategy (**Figs. 6A–C**). First, to determine whether inhibiting NTS_{POMC} neurons alters basal nociception, we conducted tail-flick and Hargreaves assays in $NTS_{POMC(Gi)}$ mice. Chemoinhibition of NTS_{POMC} neurons had no effect on tail-flick withdrawal latency (CNO 2.30 ± 0.14 vs NSS 2.37 ± 0.14 seconds, n = 6, $P = 0.51$, paired *t* test, **Figs. 6D and E**) or Hargreaves withdrawal latency (CNO 5.76 ± 0.36 vs NSS 5.7 ± 0.43 seconds, n = 6, $P = 0.90$, paired *t* test, **Figs. 6F and G**). Control animals given the same dose of CNO did not show any differences in these same tests ($NTS_{POMC(Chrim)}$, n = 6, $P > 0.05$, **Figs. 6E and G**).

It has previously been shown that stress-induced analgesia involves β-endorphin,[47] but the identity of the neurons releasing the opioid peptide has not been identified. A 3-minute swim induced analgesia with an increase in tail-flick latency (before swim 2.3 ± 0.31 vs 4.43 ± 0.33 seconds after swim, n = 8, $P = 0.0002$, **Fig. 6H**). Administration of CNO to $NTS_{POMC(Gi)}$ mice before the swim significantly attenuated the increase in tail withdrawal latency (4.43 ± 0.33 vs 3.2 ± 0.28, $P = 0.025$, RM 1-way ANOVA with Tukey post hoc test, **Fig. 6H**) returning it back toward the basal latency preswim (no longer statistically different from baseline, $P = 0.12$, Tukey post hoc test, **Fig. 6H**). Stress-induced analgesia was also observed in control $NTS_{POMC(Chrim)}$ mice (n = 4, $P = 0.01$, RM 1-way ANOVA with Tukey post hoc test) but CNO injection had no effect on this analgesic action ($P = 0.9$, Tukey post hoc test, **Fig. 6I**).

3.12. Chemogenetic inhibition of ARC_{POMC} neurons does not attenuate stress-induced analgesia

The other major site of POMC synthesis in the CNS is in the ARC (Supplemental Figure 5A-C, available at http://links.lww.com/PAIN/B733). We undertook proof of principle experiments to test whether chemogenetic inhibition of POMC neurons located in the ARC had any impact on stress analgesia. A 3-minute swim again induced a significant ($P = 0.02$) increase in tail-flick latency in $ARC_{POMC(Gi)}$ mice, but prior CNO administration did not alter this stress-induced analgesia (n = 3, $P > 0.05$, RM 1-way ANOVA with Tukey *post hoc* test, Supplemental Figure 5D-E, available at http://links.lww.com/PAIN/B733).

In all the above experiments, post hoc histology confirmed transduction of neurons with a pattern and distribution consistent with them being NTS_{POMC} or ARC $_{POMC}$ neurons (Supplemental Figure 1B and 5C, available at http://links.lww.com/PAIN/B733, **Figs. 2D, 4E, and 6C**).[13]

4. Discussion

Optogenetic or chemogenetic activation of NTS_{POMC} neurons produces a sustained analgesia that is in part mediated by endogenous opioid release. Opto-stimulation of this neuronal population also produces a transient bradycardia and bradypnoea. The chemogenetic activation of NTS_{POMC} neuron is well-tolerated by the mice as they exhibit no respiratory depression, aversion/preference, anxiolysis, or locomotor consequences. We establish that the NTS_{POMC} neurons, but not the hypothalamic ARC_{POMC} neurons, play a role in stress-induced analgesia that can be blocked by chemogenetic inhibition. This corroborates and extends our previous observations made using the PSAM chemogenetic method[13] and identifies the NTS_{POMC} neurons as a key component of endogenous analgesic circuitry.

Activation of NTS_{POMC} neurons resulted in opioid-mediated analgesia consistent with the principle that these NTS neurons release β-endorphin. Brief optoactivation of NTS_{POMC} neurons in freely behaving mice showed an analgesia action in Hargreaves and tail-flick assays that lasted for 30 minutes and was 70% to 75% blocked by naloxone. A previous study reported approximately 40% maximum possible analgesia (MPE) in tail-flick assay after morphine injection (10 mg/kg, s.c.) in mice.[10] Interestingly, in our study, if we calculate the MPE resulting from optoactivation of the NTS_{POMC} neurons in the tail-flick assay, it stands around 90%. Although this direct comparison is hampered by different study designs, nonetheless this shows a powerful endogenous analgesic effect. The presence of a residual analgesic effect (~25%) after NTS_{POMC} neuron activation after naloxone may indicate that other mechanisms besides endogenous opioids are involved or alternatively that the dose of naloxone was not sufficient to completely block the actions of focally released β-endorphin.

Using an excitatory DREADD chemogenetic approach, we again identified an opioid-mediated analgesic effect in acute pain

Copyright © 2022 by the International Association for the Study of Pain. Unauthorized reproduction of this article is prohibited.

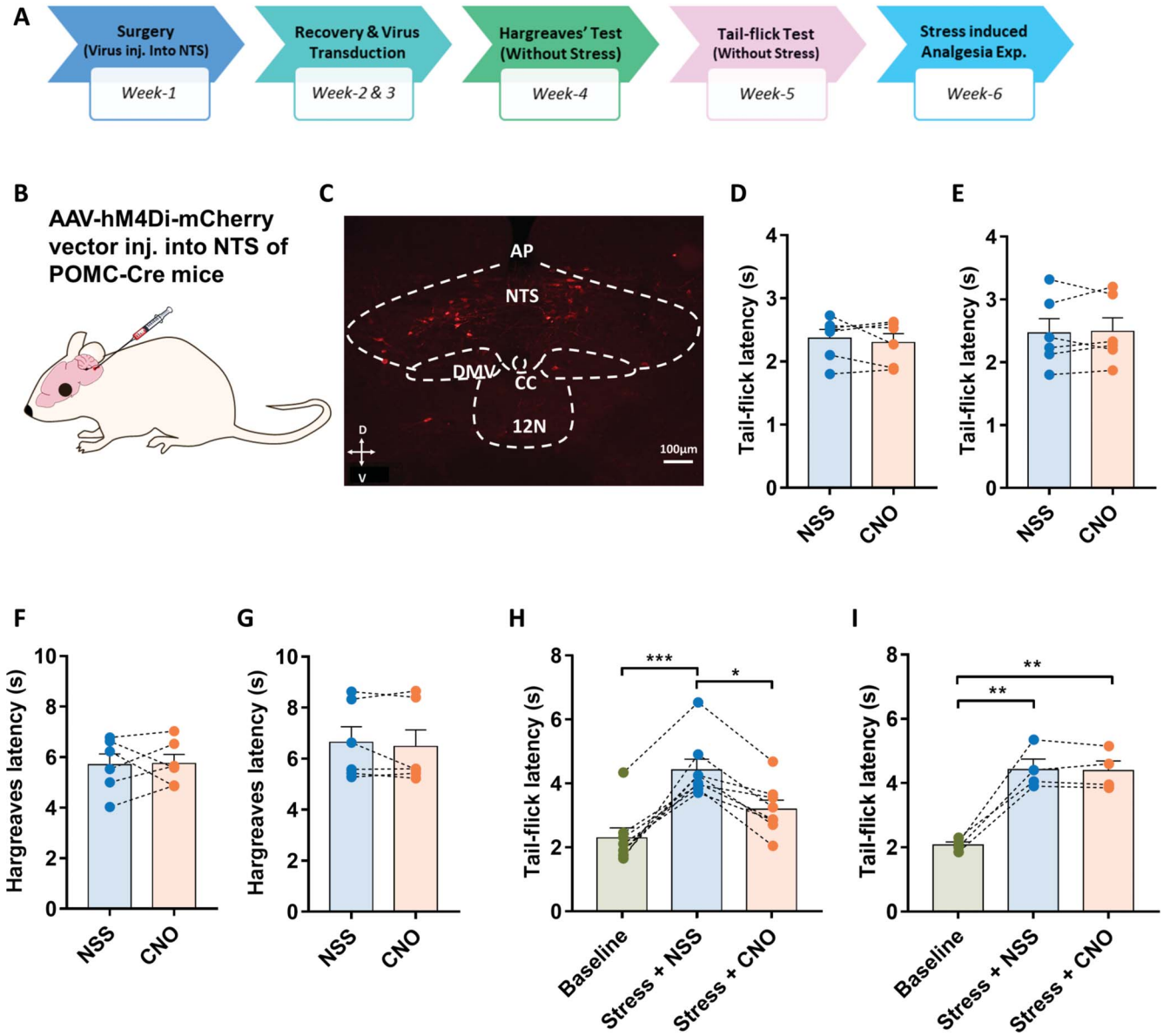


Figure 6. Effect of chemogenetic inhibition of NTS_{POMC} neurons on nociception and stress-induced analgesia. (A) Timeline for NTS_{POMC} inhibitory chemogenetic experiments. (B) Schematic diagram shows injection of AAV2 hM4Di-mcherry into the NTS of POMC-Cre mice. (C) Representative histological section of brain stem shows NTS_{POMC} neurons expressing mCherry. CNO injection (3 mg/kg, i.p.) did not produce any effect in $NTS_{POMC(Gi)}$ mice (n = 6) under basal conditions in the (D) tail-flick test or (F) Hargreaves test (paired *t* test). CNO injection to control $NTS_{POMC(Chrim)}$ mice (n = 6) showed no effect on (E) tail-flick test (same data as Fig. 4G) and (G) Hargreaves test (paired *t* test). (H) A significant increase in tail withdrawal threshold was observed in $NTS_{POMC(Gi)}$ mice after a brief swim that was attenuated by CNO injection (n = 8, RM 1-way ANOVA with Tukey post hoc test). (I) Stress-induced analgesia was also observed in $NTS_{POMC(Chrim)}$ mice and CNO failed to alter this effect (n = 4, RM 1-way ANOVA with Tukey post hoc test). Data are presented as mean ± SE.*$P < 0.05$, **$P < 0.01$ ***$P < 0.001$. AAV, adeno-associated viral vectors; ANOVA, analysis of variance; NSS, normal saline solution; NTS, nucleus of the solitary tract; POMC, pro-opiomelanocortin; DMV, Dorsal Vagal Motor Nucleus; AP Area Postrema; CC, central canal; 12N, hypoglossal.

models. These findings are in line with previous observations, using a different chemogenetic strategy, that showed NTS_{POMC} activation produced analgesia.[13] We also show that this analgesic effect is seen in an acute carrageenan model of inflammatory mechanical sensitisation but not in a neuropathic pain model. This mirrors the known beneficial actions of opioids in inflammatory pain but not neuropathic pain where they are markedly less beneficial.[17,41,58] It remains to be determined whether this apparent lack of a role in a chronic neuropathic pain model also applies to other models of chronic pain. Opioid-mediated analgesia has also been reported after electrical or direct chemical stimulation of NTS,[2,37] and our study extends these findings to indicate that focal activation of the small population of ~200 NTS_{POMC} neurons can produce powerful opioid-mediated analgesia.

β-Endorphin has been shown to play a role in stress-induced analgesia,[12,39,47] so we tested the hypothesis that NTS_{POMC} neurons may be the source of the β-endorphin that mediates stress-evoked analgesia. Chemogenetic inhibition of NTS_{POMC} neurons did not produce any change in basal nociception in both the Hargreaves and tail-flick assays, suggesting that there is no analgesic tone in the system under baseline conditions. However, inhibiting NTS_{POMC} neurons (but not those in the arcuate) attenuated swim stress–induced analgesia. This result confirms that stress-induced analgesia is mediated by β-endorphin and identified the NTS_{POMC} as a core node in the network. The NTS is

Copyright © 2022 by the International Association for the Study of Pain. Unauthorized reproduction of this article is prohibited.

a key integrating station for afferents from the viscera and from muscles[11] and is therefore well positioned to co-ordinate and mediate exercise-induced changes in sensory processing. The NTS_{POMC} neurons project into the region of the rostro-medial medulla as well as up to the ventral periaqueductal grey,[13] which would be a potential link for the NTS_{POMC} neurons into the descending pain modulation system.[40] It is also possible that these neurons could play a role in vagal stimulation-evoked analgesia[1] that is increasingly used as a therapeutic treatment for pain conditions like migraine,[49,52] but this remains to be tested.

Optoactivating NTS_{POMC} neurons produced transient bradycardia in vivo with similar characteristics to that found in the working heart–brainstem preparation.[13] Naloxone reduced the effect of opto-stimulation, which suggests that the bradycardia was in part opioid-mediated and likely because of release of β-endorphin. The NTS_{POMC} neurons project to nucleus ambiguus (NA) in close proximity to the cholinergic cardiac vagal preganglionic neurons (CVNs).[13,55] The excitation of CVNs with vagal activation can generate a bradycardia.[8,26,42] Opioids characteristically inhibit postsynaptic neurons via their cognate G-protein–coupled receptors,[16,28] and so this is not consistent with a direct synapse from NTS_{POMC} neurons directly onto CVNs. However, a fast inhibition of CVNs by adjacent interneurons has been reported.[18] Additionally, such GABAergic/glycinergic interneurons have been shown to be inhibited by exogenous opioids in vitro.[20,54] This suggests a potential mechanism whereby β-endorphins released from the POMC neurons inhibit the presynaptic inhibitory interneurons to disinhibit the CVNs and cause bradycardia. There is also evidence for glutamate-expressing POMC neurons in the arcuate nucleus of the hypothalamus.[22,27] Therefore, it is also plausible that the bradycardia seen after activation of NTS_{POMC} neurons could be because of a dual mechanism involving direct glutamatergic excitation and β-endorphin–mediated disinhibition. Distinguishing between these circuit hypotheses will likely require cellular resolution recording studies from vagal preganglionic neurons.

Because we observed transient respiratory pauses after synchronous opto-stimulation of NTS_{POMC} neurons (similar to that seen in the working heart–brainstem preparation),[13] we aimed to assess if chemogenetic activation also produced respiratory depression. Spirometry showed no sign of changes in minute volume after activation of the NTS_{POMC} neurons with a CNO dose that produced analgesia. The axons of the NTS_{POMC} neurons are known to be distributed across the ventral respiratory column and ascend to the vicinity of the Kölliker–Fuse nucleus,[13,55] both of which are known to be involved in opioid-mediated regulation of respiratory pattern.[36,44] Therefore, the necessary connectivity for these respiratory actions is present and it is likely that the difference in respiratory effects between optogenetic and chemogenetic activation relates to the pattern of activity that is triggered. Optoactivation imposes an abrupt synchronous discharge of the NTS_{POMC} neurons at an exogenous, arbitrary frequency. In contrast, the chemogenetic activation modulates the excitability of the NTS_{POMC} neurons augmenting their natural firing pattern that may be less likely to produce the respiratory suppression. Chemogenetic activation does produce an opioid-like analgesic effect likely via the release of β-endorphin, so the lack of respiratory depression cannot be explained on the basis of a differential release of opioid by each stimulation mechanism. This may indicate that there is a therapeutic window for chemogenetic activation of NTS_{POMC} neurons that reduces the risk of respiratory depression.

Our study used optogenetic and chemogenetic approaches to alter the intrinsic activity of the POMC neurons. Such approaches require controls both within animal and across groups to take account of potential off-target effects of chemogenetic ligand or nonspecific effects of blue light. We designed an efficient control group strategy using a similar AAV vector to express the chemogenetic actuator and a fluorophore for the optogenetic experiments and vice versa for chemogenetic experiments. This provided control for the effects of vector infection, expression of membrane bound actuator protein and fluorophore, and enabled blinding of experimenters. This approach offers advantages over the more commonly used strategy of just expressing a fluorophore using a Cre-dependent AAV. Our approach, however, introduces a possible confound that the actuator expression in the control group may change the excitability/function of the POMC neurons under basal conditions.[19,48] We found no evidence of changes in between-group comparisons across multiple measures; however, to rule out this possibility, we definitively would require detailed cellular electrophysiology, which was beyond the scope of our study. We also note that throughout the study there was consistency between approaches using the different optogenetic and chemogenetic actuators to change the activity in the POMC neurons, which would not have been expected if expression of the actuators was having a detrimental effect on function.

Systemic opioids are associated with a spectrum of other serious side effects besides respiratory depression, including addiction linked to reward, sedation, and anxiolysis as well as nausea and aversion/dysphoria.[16] Therefore, we sought to assess whether there was any evidence for similar actions with activation of NTS_{POMC} neurons. We found no evidence of either preference or aversion from the optoactivation or chemoactivation in the conditioned place preference assays, which suggest that activation of these neurons does not produce a strong affective valence. Similarly, in the open field test, there were no changes in either the time spent in the central zone of the arena (a measure of anxiety) or in the total distance travelled after chemoactivation. These null findings in assays of preference, anxiety-like behaviour, and locomotor behaviour from levels of activation that produced analgesic effects again are consistent with the idea that focal opioid release produced by direct activation of an opioid-releasing circuit can minimise unwanted effects. This is analogous to a more selective version of deep brain stimulation which has been shown to focally release opioids in the periaqueductal gray,[50] without some of the typical side effects seen with systemic opioids.

5. Conclusion

Overall, our study shows that opto-stimulation of NTS_{POMC} neurons produces transient cardiorespiratory depression in anaesthetised mice. We demonstrate that both optogenetic and chemogenetic activation of NTS_{POMC} neurons produces a sustained strong analgesia without evidence of adverse effects. We also provide evidence that this small population of medullary POMC neurons plays a central role in stress-induced analgesia.

Conflict of interest statement

The authors have no conflicts of interest to declare.

Copyright © 2022 by the International Association for the Study of Pain. Unauthorized reproduction of this article is prohibited.

Acknowledgements

This work was funded by Medical Research Council (ref: MR/P025749/1). For the purpose of open access, the author has applied a Creative Commons Attribution (CC BY) public copyright licence to any Author Accepted Manuscript (AAM) version arising from this submission. The source data for the paper is openly available from data.bris at DOI 10.5523/bris.3mricoucwoop82-ka13go8scs26. A. E. Pickering has grant funding from Eli Lilly and provided consultancy to Eli Lilly and Lateral Pharma unrelated to this study.

Appendix A. Supplemental digital content

Supplemental digital content associated with this article can be found online at http://links.lww.com/PAIN/B733.

Article history:
Received 30 October 2021
Received in revised form 18 September 2022
Accepted 27 September 2022
Available online 18 October 2022

References

[1] Aicher SA, Lewis SJ, Randich A. Antinociception produced by electrical stimulation of vagal afferents: independence of cervical and subdiaphragmatic branches. Brain Res 1991;542:63–70.
[2] Aicher SA, Randich A. Antinociception and cardiovascular responses produced by electrical stimulation in the nucleus tractus solitarius, nucleus reticularis ventralis, and the caudal medulla. PAIN 1990;42:103–19.
[3] Anderson EJP, Cakir I, Carrington SJ, Cone RD, Ghamari-Langroudi M, Gillyard T, Gimenez LE, Litt MJ. 60 years of POMC: regulation of feeding and energy homeostasis by alpha-MSH. J Mol Endocrinol 2016;56:T157–74.
[4] Baizman ER, Cox BM. Endorphin in rat pituitary glands: its distribution within the gland, and age related changes in gland content in male and female rats. Life Sci 1978;22:519–25.
[5] Balthasar N, Coppari R, McMinn J, Liu SM, Lee CE, Tang V, Kenny CD, McGovern RA, Chua SC Jr, Elmquist JK, Lowell BB. Leptin receptor signaling in POMC neurons is required for normal body weight homeostasis. Neuron 2004;42:983–91.
[6] Balthasar N, Dalgaard LT, Lee CE, Yu J, Funahashi H, Williams T, Ferreira M, Tang V, McGovern RA, Kenny CD, Christiansen LM, Edelstein E, Choi B, Boss O, Aschkenasi C, Zhang CY, Mountjoy K, Kishi T, Elmquist JK, Lowell BB. Divergence of melanocortin pathways in the control of food intake and energy expenditure. Cell 2005;123:493–505.
[7] Bicknell AB. The tissue-specific processing of pro-opiomelanocortin. J Neuroendocrinology 2008;20:692–9.
[8] Bieger D, Hopkins DA. Viscerotopic representation of the upper alimentary tract in the medulla oblongata in the rat: the nucleus ambiguus. J Comp Neurol 1987;262:546–62.
[9] Boecker H, Sprenger T, Spilker ME, Henriksen G, Koppenhoefer M, Wagner KJ, Valet M, Berthele A, Tolle TR. The runner's high: opioidergic mechanisms in the human brain. Cereb Cortex 2008;18:2523–31.
[10] Bohn LM, Lefkowitz RJ, Caron MG. Differential mechanisms of morphine antinociceptive tolerance revealed in βArrestin-2 knock-out mice. J Neurosci 2002;22:10494–500.
[11] Boscan P, Pickering AE, Paton JFR. The nucleus of the solitary tract: an integrating station for nociceptive and cardiorespiratory afferents. Exp Physiol 2002;87:259–66.
[12] Butler RK, Finn DP. Stress-induced analgesia. Prog Neurobiol 2009;88:184–202.
[13] Cerritelli S, Hirschberg S, Hill R, Balthasar N, Pickering AE. Activation of brainstem pro-opiomelanocortin neurons produces opioidergic analgesia, bradycardia and bradypnoea. PLoS One 2016;11:e0153187.
[14] Chaplan SR, Bach FW, Pogrel JW Chung JM & Yaksh TL. Quantitative assessment of tactile allodynia in the rat paw. J Neurosci Methods 1994;53:55–63.
[15] Contet C, Gavériaux-Ruff C, Matifas A, Caradec C, Champy MF, Kieffer BL. Dissociation of analgesic and hormonal responses to forced swim stress using opioid receptor knockout mice. Neuropsychopharmacology 2006;31:1733–44.
[16] Corbett AD, Henderson G, McKnight AT, Paterson SJ. 75 years of opioid research: the exciting but vain quest for the Holy Grail. Br J Pharmacol 2006;147(suppl 1):S153–62.
[17] Finnerup NB, Attal N, Haroutounian S, McNicol E, Baron R, Dworkin RH, Gilron I, Haanpaa M, Hansson P, Jensen TS, Kamerman PR, Lund K, Moore A, Raja SN, Rice ASC, Rowbotham M, Sena E, Siddall P, Smith BH, Wallace M. Pharmacotherapy for neuropathic pain in adults: a systematic review and meta-analysis. Lancet Neurol 2015;14:162–73.
[18] Frank JG, Jameson HS, Gorini C, Mendelowitz D. Mapping and identification of GABAergic neurons in transgenic mice projecting to cardiac vagal neurons in the nucleus ambiguus using photo-uncaging. J Neurophysiol 2009;101:1755–60.
[19] Goutaudier R, Coizet V, Carcenac C, Carnicella S. DREADDs: the power of the lock, the weakness of the key. Favoring the pursuit of specific conditions rather than specific ligands. eNeuro 2019;6:ENEURO.0171-19.2019.
[20] Griffioen KJ, Venkatesan P, Huang ZG, Wang X, Bouairi E, Evans C, Gold A, Mendelowitz D. Fentanyl inhibits GABAergic neurotransmission to cardiac vagal neurons in the nucleus ambiguus. Brain Res 2004;1007:109–15.
[21] Hargreaves K, Dubner R, Brown F, Flores C, Joris J. A new and sensitive method for measuring thermal nociception in cutaneous hyperalgesia. PAIN 1988;32:77–88.
[22] Hentges ST, Otero-Corchon V, Pennock RL, King CM, Low MJ. Proopiomelanocortin expression in both GABA and glutamate neurons. J Neurosci 2009;29:13684–90.
[23] Hughes S, Hickey L, Donaldson LF, Lumb BM, Pickering AE. Intrathecal reboxetine suppresses evoked and ongoing neuropathic pain behaviours by restoring spinal noradrenergic inhibitory tone. PAIN 2015;156:328–34.
[24] Hughes SW, Hickey L, Hulse RP, Lumb BM, Pickering AE. Endogenous analgesic action of the pontospinal noradrenergic system spatially restricts and temporally delays the progression of neuropathic pain following tibial nerve injury. PAIN 2013;154:1680–90.
[25] Huo L, Grill HJ, Bjørbæk C. Divergent regulation of proopiomelanocortin neurons by leptin in the nucleus of the solitary tract and in the arcuate hypothalamic nucleus. Diabetes 2006;55:567–73.
[26] Izzo PN, Deuchars J, Spyer KM. Localization of cardiac vagal preganglionic motoneurones in the rat: immunocytochemical evidence of synaptic inputs containing 5-hydroxytryptamine. J Comp Neurol 1993;327:572–83.
[27] Jarvie BC, Hentges ST. Expression of GABAergic and glutamatergic phenotypic markers in hypothalamic proopiomelanocortin neurons. J Comp Neurol 2012;520:3863–76.
[28] Jordan BA, Cvejic S, Devi LA. Opioids and their complicated receptor complexes. Neuropsychopharmacology 2000;23:S5–S18.
[29] Klapoetke NC, Murata Y, Kim SS, Pulver SR, Birdsey-Benson A, Cho YK, Morimoto TK, Chuong AS, Carpenter EJ, Tian Z, Wang J, Xie Y, Yan Z, Zhang Y, Chow BY, Surek B, Melkonian M, Jayaraman V, Constantine-Paton M, Wong GKS, Boyden ES. Independent optical excitation of distinct neural populations. Nat Methods 2014;11:338–46.
[30] Krashes MJ, Koda S, Ye C, Rogan SC, Adams AC, Cusher DS, Maratos-Flier E, Roth BL, Lowell BB. Rapid, reversible activation of AgRP neurons drives feeding behavior in mice. J Clin Invest 2011;121:1424–8.
[31] Lee BH, Won R, Baik EJ, Lee SH, Moon CH. An animal model of neuropathic pain employing injury to the sciatic nerve branches. Neuroreport 2000;11:657–61.
[32] Lewis JW, Baldrighi G, Akil H. A possible interface between autonomic function and pain control: opioid analgesia and the nucleus tractus solitarius. Brain Res 1987;424:65–70.
[33] Magnus CJ, Lee PH, Atasoy D, Su HH, Looger LL, Sternson SM. Chemical and genetic engineering of selective ion channel-ligand interactions. Science 2011;333:1292–6.
[34] McCarson KE, Fehrenbacher JC. Models of inflammation: carrageenan- or complete freund's adjuvant (CFA)-Induced edema and hypersensitivity in the rat. Curr Protoc 2021;1:e202.
[35] Millan MJ. Multiple opioid systems and pain. PAIN 1986;27:303–47.
[36] Montandon G, Qin W, Liu H, Ren J, Greer JJ, Horner RL. PreBotzinger complex neurokinin-1 receptor-expressing neurons mediate opioid-induced respiratory depression. J Neurosci 2011;31:1292–301.
[37] Morgan MM, Sohn JH, Lohof AM, Ben-Eliyahu S, Liebeskind JC. Characterization of stimulation-produced analgesia from the nucleus tractus solitarius in the rat. Brain Res 1989;486:175–80.
[38] Morgan WP. Affective beneficence of vigorous physical activity. Med Sci Sports Exerc 1985;17:94–100.
[39] Nakagawasai O, Tadano T, Tan No K, Niijima F, Sakurada S, Endo Y, Kisara K. Changes in beta-endorphin and stress-induced analgesia in mice after exposure to forced walking stress. Methods Find Exp Clin Pharmacol 1999;21:471–6.

Copyright © 2022 by the International Association for the Study of Pain. Unauthorized reproduction of this article is prohibited.

[40] Ossipov MH, Dussor GO, Porreca F. Central modulation of pain. J Clin Invest 2010;120:3779–87.
[41] Ossipov MH, Kovelowski CJ, Porreca F. The increase in morphine antinociceptive potency produced by carrageenan-induced hindpaw inflammation is blocked by naltrindole, a selective delta-opioid antagonist. Neurosci Lett 1995;184:173–6.
[42] Palkovits M, Mezey E, Eskay RL. Pro-opiomelanocortin-derived peptides (ACTH/β-endorphin/α-MSH) in brainstem baroreceptor areas of the rat. Brain Res 1987;436:323–38.
[43] Pisanello F, Mandelbaum G, Pisanello M, Oldenburg IA, Sileo L, Markowitz JE, Peterson RE, Della Patria A, Haynes TM, Emara MS, Spagnolo B, Datta SR, De Vittorio M, Sabatini BL. Dynamic illumination of spatially restricted or large brain volumes via a single tapered optical fiber. Nat Neurosci 2017;20:1180–8.
[44] Prkic I, Mustapic S, Radocaj T, Stucke AG, Stuth EAE, Hopp FA, Dean C, Zuperku EJ. Pontine μ-opioid receptors mediate bradypnea caused by intravenous remifentanil infusions at clinically relevant concentrations in dogs. J Neurophysiol 2012;108:2430–41.
[45] Radosevich PM, Nash JA, Brooks Lacy D, O'Donovan C, Williams PE, Abumrad NN. Effects of low- and high-intensity exercise on plasma and cerebrospinal fluid levels of ir-beta-endorphin, ACTH, cortisol, norepinephrine and glucose in the conscious dog. Brain Res 1989;498: 89–98.
[46] Roth BL. DREADDs for neuroscientists. Neuron 2016;89:683–94.
[47] Rubinstein M, Mogil JS, Japon M, Chan EC, Allen RG, Low MJ. Absence of opioid stress-induced analgesia in mice lacking beta-endorphin by site-directed mutagenesis. Proc Natl Acad Sci U S A 1996;93: 3995–4000.
[48] Saloman JL, Scheff NN, Snyder LM, Ross SE, Davis BM, Gold MS. Gi-DREADD expression in peripheral nerves produces ligand-dependent analgesia, as well as ligand-independent functional changes in sensory neurons. J Neurosci 2016;36:10769–81.
[49] Silberstein SD, Calhoun AH, Lipton RB, Grosberg BM, Cady RK, Dorlas S, Simmons KA, Mullin C, Liebler EJ, Goadsby PJ, Saper JR. Chronic migraine headache prevention with noninvasive vagus nerve stimulation: the EVENT study. Neurology 2016;87:529–38.
[50] Sims-Williams H, Matthews JC, Talbot PS, Love-Jones S, Brooks JC, Patel NK, Pickering AE. Deep brain stimulation of the periaqueductal gray releases endogenous opioids in humans. Neuroimage 2017;146: 833–42.
[51] Stein L, Belluzzi JD. Brain endorphins: possible role in reward and memory formation. Fed Proc 1979;38:2468–72.
[52] Tassorelli C, Grazzi L, de Tommaso M, Pierangeli G, Martelletti P, Rainero I, Dorlas S, Geppetti P, Ambrosini A, Sarchielli P, Liebler E, Barbanti P. Noninvasive vagus nerve stimulation as acute therapy for migraine: the randomized PRESTO study. Neurology 2018;91:e364–73.
[53] van den Pol AN, Acuna C, Davis JN, Huang H, Zhang X. Defining the caudal hypothalamic arcuate nucleus with a focus on anorexic excitatory neurons. J Physiol 2019;597:1605–25.
[54] Venkatesan P, Baxi S, Evans C, Neff R, Wang X, Mendelowitz D. Glycinergic inputs to cardiac vagal neurons in the nucleus ambiguus are inhibited by nociceptin and mu-selective opioids. J Neurophysiol 2003; 90:1581–8.
[55] Wang D, He X, Zhao Z, Feng Q, Lin R, Sun Y, Ding T, Xu F, Luo M, Zhan C. Whole-brain mapping of the direct inputs and axonal projections of POMC and AgRP neurons. Front Neuroanat 2015;9:40.
[56] Yizhar O, Fenno LE, Davidson TJ, Mogri M, Deisseroth K. Optogenetics in neural systems. Neuron 2011;71:9–34.
[57] Zhan C, Zhou J, Feng Q, Zhang JE, Lin S, Bao J, Wu P, Luo M. Acute and long-term suppression of feeding behavior by POMC neurons in the brainstem and hypothalamus, respectively. J Neurosci 2013;33:3624–32.
[58] Zhang X-Y, Dou Y-N, Yuan L, Li Q, Zhu Y-J, Wang M, Sun Y-G. Different neuronal populations mediate inflammatory pain analgesia by exogenous and endogenous opioids. eLife 2020;9:e55289.

Copyright © 2022 by the International Association for the Study of Pain. Unauthorized reproduction of this article is prohibited.